Discussion

This is a systematic study to reveal the clinical characteristics of EOD in consecutive patients over a period of 8 years at a memory clinic in Japan. It is worthy of notice that nearly 30% of the demented patients had an age of onset of less than 65 years.

Comparing with other studies in Japan, Miyanaga et al. [14] estimated that there are a total of 25,000 EOD patients (32 patients per 100,000 population) in Japan, only a few percent of more than 2 million demented patients. Yokota et al. [15] reported that only 34 patients (7.3%) had an age of onset of less than 65 years out of a total of 464 demented patients from their outpatients of psychiatric hospitals in Japan. Both studies showed a much fewer number of EOD patients than our study. Comparing with other countries, Harvey et al. [5] estimated that there are 54 EOD patients per 100,000 population in their epidemiological study in the UK, almost the same number as the one previously reported in Japan. An outpatient study in Denmark showed that a total of 314 patients per 1,000 demented patients were aged less than 60 years [4], an outpatient study in the USA reported that 29.3% of 948 demented patients were EOD patients [16], and a UK study showed that the proportion of EOD patients was 28.6% [17]. All these results are consistent with our result. An outpatient study in Brazil showed that 46.6% of all demented patients were EOD patients [18], a relatively high number compared to other studies. There may be more EOD patients in Japan than previously reported.

In our study, the sex ratio in the EOD group was almost equal, whereas there were more females in the LOD group. In fact, many epidemiological studies revealed that there were more female patients among the demented elderly [19–21], while there were more males among EOD patients [5, 14]. This may be because there are more male-related causes of dementia, such as VaD or alcohol-related dementia, in EOD groups. There is a possibility that the sex ratio of AD is affected by onset age, as some studies mentioned that there are more males in early-onset AD patients than in late-onset AD patients [3].

The education level was significantly higher in EOD groups. This may be due to changes in the educational system in Japan after World War II.

As there were no significant differences between the EOD and LOD groups in CDR and MMSE score at the first consultation, we performed this analysis with all causes of dementia together; however, cognitive function and severity of dementia could not be discussed for each cause of dementia. Therefore, further assessments are needed on cognitive function and psychiatric symptoms for all causes of dementia.

It is noteworthy that in EOD patients the duration from disease onset to consultation is longer than in LOD patients. Therefore, it seems that the progress of dementia in EOD patients is slow, even though the severity of dementia is equal between the two groups. However, in patients with AD, which is the major cause of dementia, early-onset groups are known to show a more rapid progression than late-onset groups [22, 23]. Therefore, we suppose that in EOD patients it takes longer to correctly diagnose the disease because early-onset patients are sometimes misdiagnosed as having psychiatric disorders such as schizophrenia or mood disorders. Furthermore, EOD groups consist of not only patients with neurodegenerative disorders or cerebrovascular diseases but also of patients with many heterogeneous causes of dementia, such as TBI or neurosyphilis. These pathologies sometimes require more time to be diagnosed by specialists in dementia. This misdiagnosis might have led to the under-recognition of EOD, and hence, to the underestimation of its prevalence. This issue is important from a socioeconomic point of view, and we need to inform people further about EOD.

There are also a few noteworthy findings in the classification of causes of dementia in our study. Among our patients, 12.6% of all EOD patients had VaD and there was no significant difference between that number and the number of LOD patients (9.7%). Although several epidemiological studies have reported that VaD was more common in patients aged less than 65 years compared with elderly patients [3, 18, 24], our result was not consistent with these findings. The distribution of the diagnoses of VaD is influenced by the specificity and sensitivity of the criteria used in each study, and the NINDS-AIREN criteria are known to be the strictest criteria, requesting onset of dementia within 3 months following a recognized stroke [25, 26]. This low prevalence of VaD in our study may be because we used the NINDS-AIREN criteria to diagnose VaD, and young patients may not have recognized their strokes. Furthermore, as our series of patients are outpatients of the neuropsychiatry department, there is a possibility that there might be few subjects with clear neurological symptoms due to cardiovascular disease.

Among our patients, DLB was the second most common cause of dementia (10.9%) in the LOD group while there were only a few DLB patients (0.5%) in the EOD group. Although there were little epidemiological data on clinically diagnosed DLB compared with research on au-

topsy patients, some investigations on EOD reported a low prevalence of DLB patients [4, 5, 27]. These findings suggest that the onset age of DLB seems to be considerably old.

Among our patients, FTLD was the second most common cause of dementia following AD among the EOD group (21.4%; AD/FTLD = 1.8:1) while it was relatively rare among the late-onset patients (4.9%; AD/FTLD = 12.5:1). Although this rate of FTLD in the EOD group is higher than in other studies in Japan [14, 15], it is not a surprising rate compared with those in other countries. Many studies in Western countries report that FTLD is the second most common cause of dementia following AD among early-onset patients [6, 28–30]. An epidemiological study in the UK showed that the rate of FTLD was 15.7% out of a total of 108 demented people aged <65 years, whereas the rate of AD was 25% (FTD/AD = 1:1.6) [29]. Although there are some familial and genetic cases among FTLD patients in Western countries and the pathoetiologic background of FTLD in Japan may be different from that in Western countries [28, 31], our results suggest that FTLD in Japan has been underestimated until now.

Turning to the changes of the proportion of subjects during the three sequential research periods, there were no significant differences between either demented subjects and nondemented subjects or between EOD patients and LOD patients. This result suggests that the proportion of EOD and LOD patients was not affected by the recent trend of increased awareness of dementia, although the number of all patients increased. Moreover, the severity of dementia at the first consultation did not differ during the research period. This may suggest that early diagnosis and early referral are still not enough even today. Further information about dementia for families and for general physicians is required.

There are a few methodological issues that should be taken into consideration to fully appreciate our results. Firstly, this study is based on memory clinic patients in the department of neuropsychiatry of a university hospital, thus it is not a purely community-based epidemiological study. Referral bias may affect the proportion of each diagnosis in this study. Relatively common causes of dementia such as AD or VaD may be treated by general physicians, and physicians may refer patients with aphasia or motor neuron symptoms to other neurological referral centers. Younger patients may be threatened with loss of employment due to dementia, which may lead the family and the general physician to refer the patient to a specialist. Older patients may have less opportunity of referral because of their age. This possible selection bias may affect the proportions of EOD and LOD patients. However, as we mentioned above, pure cross-sectional or population studies are impractical for rare diseases, and many epidemiological studies of dementia are intended for people over 65 years of age. Therefore, an assessment of a large number of consecutive patients at a memory clinic might be important. Furthermore, as our clinic is one of the few specialized clinics for demented people in our regional area where we can evaluate patients with MRI and HMPAO-SPECT, we believe our result is not inaccurate. Secondly, determining the age of onset and the duration of degenerative dementia is difficult. This study is based on the retrospective recall of caregivers, and it can be claimed that the informants' memories may have been inaccurate. Thirdly, in this study we clinically diagnosed AD, VaD, DLB, FTLD and other causes of dementia according to consensus diagnostic criteria. We did not perform pathological confirmations, so we cannot discuss the pathological background of our diagnoses. However, we routinely used the Neuropsychiatric Inventory [32] and Stereotypy Rating Inventory [33] for all patients in order to assess the psychiatric and behavioral symptoms of the patients. Moreover, we used a comprehensive frontal function assessment battery including motor series, conflicting instruction, digit span, word fluency test, trail making test, and the Stroop color-word test, for those in whom FTLD was suspected. As described previously, all patients underwent brain MRI and almost all patients underwent HMPAO-SPECT. All the patients with FTLD showed either frontal/temporal lobe atrophy on MRI, or frontal/temporal hypoperfusion on HMPAO-SPECT. Even when frontal system dysfunction was detected by neuropsychological tests in some patients with AD and VaD, they did not show frontal lobe atrophy on MRI or frontal hypoperfusion on HMPAO-SPECT. Therefore, we believe that our clinical diagnosis of the causes of dementia is the most accurate possible.

In conclusion, EOD patients are not rare, at least in memory clinics. There are many atypical causes of dementia among EOD patients such as FTLD or TBI, so clinicians have to take into consideration the specific clinical symptoms and histories of these diseases when examining such patients. Since in EOD patients the duration from their disease onset to consultation is longer, further information for the public and social support services for EOD patients are required.

References

▶1 Treves T, Korczyn AD, Zilber N, Kahana E, Leibowitz Y, Alter M, Schoenberg BS: Presenile dementia in Israel. Arch Neurol 1986;43: 26–29.

▶2 McGonigal G, Thomas B, McQuade C, Starr JM, MacLennan WJ, Whalley LJ: Epidemiology of Alzheimer's presenile dementia in Scotland, 1974–1988. BMJ 1993;306:680–683.

▶3 Newens AJ, Forster DP, Kay DW, Kirkup W, Bates D, Edwardson J: Clinically diagnosed presenile dementia of the Alzheimer type in the northern health region: ascertainment, prevalence, incidence and survival. Psychol Med 1993;23:631–644.

▶4 Vraamark Elberling T, Stokholm J, Hogh P, Waldemar G: Diagnostic profile of young and middle-aged memory clinic patients. Neurology 2002;59:1259–1262.

▶5 Harvey RJ, Skelton-Robinson M, Rosser MN: The prevalence and causes of dementia in people under the age of 65 years. J Neurol Neurosurg Psychiatry 2003;74:1206–1209.

6 Harvey RJ: Epidemiology of presenile dementia; in Hodges JR (ed): Early-Onset Dementia. A Multidisciplinary Approach. New York, Oxford University Press, 2001, pp 1–22.

▶7 Folstein MF, Folstein SE, McHugh PR: Mini-mental state: a practical method for grading the cognitive state of patients for clinician. J Psychiatr Res 1975;12:189–198.

▶8 Hughes CP, Berg L, Danziger WL, Coben LA, Martin RL: A new clinical scale for the staging of dementia. Br J Psychiatry 1982; 140:566–572.

9 American Psychiatric Association: Diagnostic and Statistical Manual of Mental Disorders, ed 3 revised. Washington, American Psychiatric Association, 1987.

▶10 McKhann G, Drachman D, Folstein M, Katzman R, Price D, Stadlan EM: Clinical diagnosis of Alzheimer's disease: report of the NINCDS-ADRDA Work Group under the auspices of Department of Health and Human Services Task Force on Alzheimer's Disease. Neurology 1984;34:939–944.

▶11 Roman GC, Tatemichi TK, Erkinjuntti T, Cummings JL, Masdeu JC, Garcia JH, Amaducci L, Orgogozo JM, Brun A, Hofman A, et al: Vascular dementia: diagnostic criteria for research studies. Report of the NINDS-AIREN International Workshop. Neurology 1993;43:250–260.

▶12 McKeith IG, Galasko D, Kosaka K, Perry EK, Dickson DW, Hansen LA, Salmon DP, Lowe J, Mirra SS, Byrne EJ, Lennox G, Quinn NP, Edwardson JA, Ince PG, Bergeron C, Burns A, Miller BL, Lovestone S, Collerton D, Jansen EN, Ballard C, de Vos RA, Wilcock GK, Jellinger KA, Perry RH: Consensus guidelines for the clinical and pathologic diagnosis of dementia with Lewy bodies (DLB): report of the consortium on DLB international workshop. Neurology 1996;47:1113–1124.

▶13 Neary D, Snowden JS, Gustafson L, Passant U, Stuss D, Black S, Freedman M, Kertesz A, Robert PH, Albert M, Boone K, Miller BL, Cummings J, Benson DF: Frontotemporal lobar degeneration: a consensus on clinical diagnostic criteria. Neurology 1998;51: 1546–1554.

14 Miyanaga K, Yonemura K, Ichinowatari N, Otuska T, Kasahara H, Kumamoto T, Kori N, Chiba H, Nagase T, Nagai M, Nishijima H, Yamazaki M: Epidemiological study of dementia in the period of 18–64 years in Japan (in Japanese). Jap J Geriat Psychiatry 1997;8: 1317–1331.

▶15 Yokota O, Sasaki K, Fujisawa Y, Takahashi J, Terada S, Ishihara T, Nakashima H, Kugo A, Ata T, Ishizu H, Kuroda S: Frequency of early- and late-onset dementias in a Japanese memory disorders clinic. Eur J Neurol 2005; 12:782–790.

▶16 McMurtray A, Christine, D, Mendez MF: Early-onset dementia: frequency and causes compared to late-onset dementia. Dement Geriatr Cogn Disord 2006;21:59–64.

17 Harvey RJ, Rossor MN, Skelton-Robinson M: Young Onset Dementia: Epidemiology, Clinical Symptoms, Family Burden, Support and Outcome. London, Dementia Research Group, 1998, http://www.dementia.ion-ucl.ac.uk.

▶18 Fujihara S, Brucki SM, Rocha MS, Carvalho AA, Piccolo AC: Prevalence of presenile dementia in a tertiary outpatient clinic. Arq Neuropsiquiatr 2004;62:592–595.

▶19 Hofman A, Rocca WA, Brayne C, Breteler MM, Clarke M, Cooper B, Copeland JR, Dartigues JF, da Silva Droux A, Hagnell O, et al: The prevalence of dementia in Europe: a collaborative study of 1980–1990 findings. Eurodem Prevalence Research Group. Int J Epidemiol 1991;20:736–748.

▶20 Ott A, Breteler MM, van Harskamp F, Stijnen T, Hofman A: Incidence and risk of dementia. The Rotterdam Study. Am J Epidemiol 1998;147:574–580.

▶21 Andersen K, Launer LJ, Dewey ME, Letenneur L, Ott A, Copeland JR, Dartigues JF, Kragh-Sorensen P, Baldereschi M, Brayne C, Lobo A, Martinez-Lage JM, Stijnen T, Hofman A: Gender differences in the incidence of AD and vascular dementia: The EURODEM Studies. EURODEM Incidence Research Group. Neurology 1999;53:1992–1997.

▶22 Huff FJ, Growdon JH, Corkin S, Rosen TJ: Age at onset and rate of progression of Alzheimer's disease. J Am Geriatr Soc 1987; 35:27–30.

▶23 Jacobs D, Sano M, Marder K, Bell K, Bylsma F, Lafleche G, Albert M, Brandt J, Stern Y: Age at onset of Alzheimer's disease: relation to pattern of cognitive dysfunction and rate of decline. Neurology 1994;44:1215–1220.

▶24 Woodburn KJ, Johnstone EC: Early-onset dementia in Lothian, Scotland: an analysis of clinical features and patterns of decline. Health Bull 1999;57:384–392.

▶25 Chui HC, Victoroff JI, Margolin D, Jagust W, Shankle R, Katzman R: Criteria for the diagnosis of ischemic vascular dementia proposed by the State of California Alzheimer's Disease Diagnostic and Treatment Centers. Neurology 1992;42:473–480.

▶26 Meguro K, Ishii H, Yamaguchi S, Ishizaki J, Shimada M, Sato M, Hashimoto R, Shimada Y, Meguro M, Yamadori A, Sekita Y: Prevalence of dementia and dementing diseases in Japan: the Tajiri project. Arch Neurol 2002; 59:1109–1114.

▶27 Hogh P, Waldemar G, Knudsen GM, Bruhn P, Mortensen H, Wildschiodtz G, Bech RA, Juhler M, Paulson OB: A multidisciplinary memory clinic in a neurological setting: diagnostic evaluation of 400 consecutive patients. Eur J Neurol 1999;6:279–288.

▶28 Snowden JS, Neary D, Mann DM: Frontotemporal dementia. Br J Psychiatry 2002; 180:140–143.

▶29 Ratnavalli E, Bayne C, Dawson K, Hodges JR: The prevalence of frontotemporal dementia. Neurology 2002;58:1615–1621.

▶30 Knopman DS, Petersen RC, Edland SD, Cha RH, Rocca WA: The incidence of frontotemporal lobar degeneration in Rochester, Minnesota, 1990 through 1994. Neurology 2004; 62:506–508.

▶31 Ikeda M, Ishikawa T, Tanabe H: Epidemiology of frontotemporal lobar degeneration. Dement Geriatr Cogn Disord 2004;17:265–268.

▶32 Cummings JL, Mega M, Gray K, Rosenberg-Thompson S, Carusi DA, Gornbein J: The Neuropsychiatric Inventory: comprehensive assessment of psychopathology in dementia. Neurology 1994;44:2308–2314.

▶33 Shigenobu K, Ikeda M, Fukuhara R, Maki N, Hokoishi K, Nebu A, Yasuoka T, Komori K, Tanabe H: The Stereotypy Rating Inventory for frontotemporal lobar degeneration. Psychiatry Res 2002;110:175–187.

Role of Neuroimaging in Alzheimer's Disease, with Emphasis on Brain Perfusion SPECT*

Hiroshi Matsuda

Department of Nuclear Medicine, Saitama Medical University Hospital, Saitama, Japan

Structural MRI and functional imaging by SPECT as well as ^{18}F-FDG PET are widely used in the diagnosis of Alzheimer's disease (AD). Metabolic and perfusion reductions in the parietotemporal association cortex are recognized as a diagnostic pattern for AD. Outstanding progress in the diagnostic accuracy of these modalities has been achieved with statistical analysis on a voxel-by-voxel basis after anatomic standardization of individual scans to a standardized brain volume template instead of visual inspection or a volume-of-interest technique. In a very early stage of AD, this statistical approach revealed losses of gray matter in the entorhinal and hippocampal areas and hypometabolism or hypoperfusion in the posterior cingulate cortex and precuneus. This statistical approach also offers a prediction of the conversion from mild cognitive impairment (MCI) to AD. The presence of hypometabolism or hypoperfusion in parietal association areas and entorhinal atrophy at the MCI stage have been reported to predict a rapid conversion to AD. A recent advance in voxel-based statistical analysis has markedly enhanced the value of brain perfusion SPECT in diagnosing early AD at the stage of MCI.

Key Words: Alzheimer's disease; SPECT; PET; MRI; statistical image analysis

J Nucl Med 2007; 48:1289–1300
DOI: 10.2967/jnumed.106.037218

With increasing life expectancy in much of the world, the number of older people at risk of developing dementia is growing rapidly, and Alzheimer's disease (AD) remains the most common cause of dementia in all age groups. AD is a progressive neurodegenerative disorder associated with a disruption of neuronal function and a gradual deterioration in cognition, function, and behavior. AD is pathologically characterized by the presence of amyloid deposition and neurofibrillary tangles, together with the loss of cortical neurons and synapses (*1*). The most profound and earliest cognitive deficits seem to be impairment of episodic memory—the ability to recall events that are specific to a time and place. Medications such as cholinesterase inhibitors are able to delay the progression of AD (*2*). Moreover, patients who have AD and in whom the start of cholinesterase inhibitor therapy is delayed demonstrate fewer benefits than do patients starting therapy early in the course of AD (*3*). This fact has shifted the focus of present studies on AD toward earlier diagnosis and longitudinal investigations to assess the value of therapeutic interventions.

Biomarkers are likely to be very important in these studies on AD. A clinical diagnosis of AD is inaccurate even among experienced investigators in about 10%–15% of cases, and biomarkers might improve the accuracy of diagnosis (*4*). The histopathologically confirmed sensitivity and specificity of ^{18}F-FDG PET for detecting the presence of AD were 94% and 73%, respectively, as determined by testing performed once and at an early stage of the disease (*5*). In contrast, clinical evaluation without ^{18}F-FDG PET had histopathologically confirmed sensitivity and specificity of 83%–85% and 50%–55%, respectively, as determined by an entire series of evaluations repeated over a period of years (*5*). For the development of putative disease-modifying drugs for AD, biomarkers might also serve as a surrogate endpoint of disease severity. When used in this way, biomarkers might be able to reduce sample sizes of clinical trials, and a change in a biomarker could be considered supporting evidence of disease modification.

PET, SPECT, and MRI have been used as imaging biomarkers. Recent advances in instruments have facilitated investigations of functional and structural alterations in fine structures of not only cortical but also subcortical areas with a high spatial resolution. In Japan, ^{18}F-FDG PET for the detection of dementia has not yet been accepted for reimbursement in the health insurance system, and more widely available brain perfusion SPECT and MRI mainly have been used for the imaging diagnosis of AD. Silverman (*6*) described the superiority of PET over SPECT in diagnosing early AD because of its higher sensitivity and higher spatial resolution, and ^{18}F-FDG PET indeed offers many advantages for detecting abnormalities in a brain affected by AD. SPECT offers the advantages of lower cost and ease

Received Dec. 24, 2006; revision accepted Apr. 19, 2007.
For correspondence or reprints contact: Hiroshi Matsuda, Department of Nuclear Medicine, Saitama Medical University Hospital, 38 Morohongo, Moroyama-machi, Iruma-gun, Saitama 350-0495, Japan.
E-mail: matsudah@saitama-med.ac.jp
*NOTE: FOR CE CREDIT, YOU CAN ACCESS THIS ACTIVITY THROUGH THE SNM WEB SITE (http://www.snm.org/ce_online) THROUGH AUGUST 2008.
No potential conflict of interest relevant to this article was reported.

of access, which could lead to a large increase in the number of cases being studied with this technique. Few studies have directly compared brain perfusion SPECT and ^{18}F-FDG PET in AD. Messa et al. (*7*) performed SPECT and ^{18}F-FDG PET in healthy control subjects and patients with mild to moderate AD. They reported that the 2 techniques had similar abilities for delineating reductions in perfusion and metabolism in the temporoparietal cortex and similar diagnostic accuracies. Herholz et al. (*8*) showed good correspondence between ^{18}F-FDG PET and SPECT for detecting changes in the temporoparietal cortex in mild to moderate AD by using voxel-based statistical image analysis, although ^{18}F-FDG PET demonstrated a more robust separation of patients with AD from healthy volunteers than did SPECT (*8*). Moreover, brain perfusion SPECT generally correlated with histopathologic changes in the distribution of neurofibrillary pathology in AD (*9*), although the results for the medial temporal lobe were discordant.

This review describes recent progress in the neuroimaging of AD, with an emphasis on brain perfusion SPECT.

VOXEL-BASED SPECT AND PET ANALYSES

The recent implementation of computer-assisted SPECT and PET analyses affords objective and more reliable assessments of functional abnormalities by means of stereotactic coordinates, relative to the visual interpretation of raw tomographic images. This stereotactic approach is a voxel-by-voxel analysis in the stereotactic space to avoid subjectivity and to adopt the principle of data-driven analysis. Although an alternative approach involving a volume-of-interest (VOI) technique has gained general acceptance, it is limited by the fact that the selection of a sample depends on the observer's a priori choice and hypothesis and leaves large areas of the brain unexplored.

Statistical Parametric Mapping (SPM)

SPM software (*10*) (Wellcome Department of Cognitive Neurology, University College–London) is the most widely used and evaluated image analysis software in brain imaging research. It has been widely applied for AD and at-risk groups in both cross-sectional and longitudinal analyses. It benefits from an open-source code that permits modification, including approaches that can use voxel-based regression and longitudinal growth-modeling approaches to test hypotheses on trajectories of cognitive decline. Current versions of SPM (e.g., SPM99, SPM2, and SPM5) permit anatomic standardization of SPECT or PET data either with or without MRI coregistration. For default analyses, I use the Montreal Neurologic Institute template to anatomically standardize SPECT and PET data. The image data are smoothed with a gaussian kernel that effectively reduces the number of resolution elements in the analysis. The possibility of type I error is an important consideration with the large number of statistical tests used in voxel-based analyses for a confirmatory research analysis, although correction for multiple comparisons is not necessarily used for the interpretation of clinical studies in a comparison of individual data with a control database. Statistical maps can be generated without any normalization of global intersubject differences in measures of interest or with normalization of the data for variations in measures of the whole brain or a relatively spared reference structure, such as the cerebellum or pons, by use of proportionate scaling or an analysis of covariance.

Three-Dimensional Stereotactic Surface Projection (3D-SSP)

The use of 3D-SSP (*11*) for SPECT or PET data analysis is an approach that can be performed without structural image data and that transforms SPECT and PET images to a standard stereotactic orientation. This type of analysis differs from typical SPM-based analyses in several ways, primarily by extracting data from the medial and lateral brain surfaces, helping to address the potentially confounding effects of inaccuracies in anatomic standardization, and reducing the combined effects of brain atrophy and partial-volume averaging on the images. Processing steps include the generation of sequential images that can be used for quality control of data analysis, as the first step of alignment and interpolation of images can reveal detector variations and positioning errors missed during the review of transaxial images. Subsequent steps in image analysis include centering the image volume, finding the midsagittal plane, and estimating the anterior commisura–posterior commisura line. Next, data for each brain are transformed into a standard stereotactic space, including first rigid-body translation and rotation with linear scaling and then nonlinear warping based on a thin-plate spline algorithm that makes use of iterative searches and cortical landmarks. The resulting 3-dimensional images are used to generate surface projections by sampling pixels along a vector perpendicular to a plane tangential to the cortical surface. The search starts at the cortical surface, and the depth of the search can be varied but typically is 10–15 mm. After location of the peak pixel along each vector, the value of this peak is transferred to a display format, resulting in 8 standard surface projection images: left and right lateral surface, left and right medial surface, superior surface, inferior surface, anterior surface, and posterior surface. These surface projection images are then compared with reference images for intersubject comparisons. A pixel-by-pixel comparison of these surface projection maps can then be used for intersubject comparisons with either *t* or *z* statistics. 3D-SSP has been used extensively in cross-sectional studies of dementia.

Tomographic *z* Score Mapping

In a software program that is widely used in Japan for the statistical analysis of brain perfusion SPECT data (Figs. 1 and 2) (*12–14*), voxel-by-voxel *z* score analysis after voxel normalization to global mean or cerebellar values [*z* score = (control mean − individual value)/control SD] is performed as described by Minoshima et al. (*11*). The

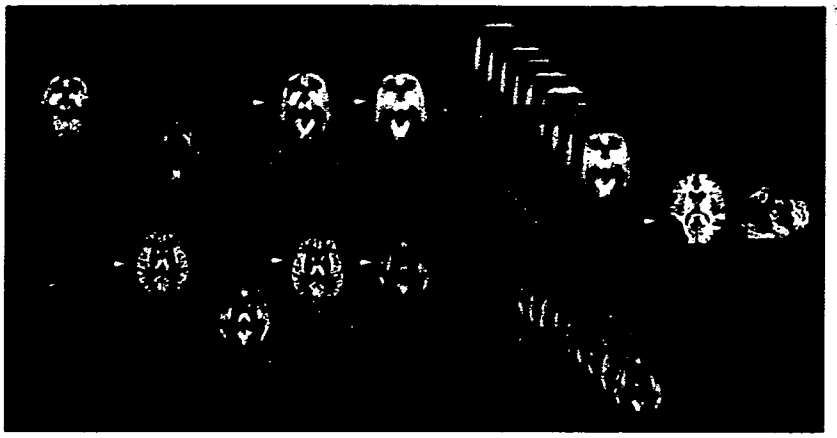

FIGURE 1. Procedures for statistical image analysis of brain perfusion SPECT and MRI data. Anatomically standardized and then smoothed SPECT or gray matter image of subject is compared with each normal database by *z* score analysis. Obtained *z* score maps are displayed by overlay on anatomically standardized MRI template.

resulting *z* score maps are displayed both by overlay on tomographic sections (not attainable with 3D-SSP) and by projection with an averaged *z* score for a 14-mm thickness to a surface rendering of the anatomically standardized MRI template. Anatomic standardization of SPECT images into a stereotactic space is performed with SPM2. It has been reported that 3D-SSP with 2-dimensional surface projection of cortical activities is less sensitive to artifacts derived from incomplete anatomic standardization of a brain with localized cortical atrophy than is SPM99 (*15*). However, on 3-dimensional location, 3D-SSP loses information that SPECT images inherently possess. This program also can incorporate SPM results into an automated analysis of *z* score values as a VOI. A specific VOI can be determined by group comparison of SPECT images for patients with a neuropsychiatric disease with those for healthy volunteers by use of SPM. In this program, a specific VOI for very early AD is incorporated to evaluate tracer uptake in the posterior cingulate gyrus, precuneus, and parietal association cortex (*14*).

Three indicators for characterizing decreases in regional cerebral blood flow (rCBF) in patients with very early AD have been determined (*14*). First, the severity of decreases in rCBF in a specific VOI showing a reduction in rCBF in very early AD is obtained from the averaged positive *z* scores in the VOI. Second, the extent of a region showing a significant reduction in rCBF in the VOI is the percentage of the coordinates with *z* values exceeding the threshold value of 2. Third, the ratio of the extent of a region showing a significant reduction in rCBF in the VOI to the extent of a region showing a significant reduction in rCBF in the whole brain is also the percentage of the coordinates with *z* values exceeding the threshold value of 2. This ratio indicates the specificity of the reduction in rCBF in the VOI relative to the whole brain.

Even if a center can construct a "normal" database with high quality and comprising a large number of healthy volunteers, other centers may not be able to use this normal database because of differences in equipment and physical correction algorithms. Because SPECT exhibits greater variations in image quality among different centers than does PET, a special technique may be necessary for sharing a normal database for SPECT. A trial with a Hoffman 3-dimensional brain phantom experiment was conducted to attempt to determine systematic differences between SPECT scanners (*12*). SPECT images for the same brain phantom were obtained with 2 different scanners. Dividing these 2 phantom images after anatomic standardization by SPM created a 3-dimensional conversion map. This conversion map was applied to convert an anatomically standardized SPECT image obtained with one scanner to that obtained with the other scanner. Although the SPM demonstrated clinically adequate validity for this conversion (*12*), further validation is required.

VOXEL-BASED MRI ANALYSIS

Volumetric MRI has become increasingly important in the study of AD, particularly as an aid to diagnosis and as a biomarker of disease progression. It is often difficult to evaluate mild atrophy of a region in AD by visual inspection of MR images. On the other hand, volumetric assessment on MRI in routine clinical practice is precluded by the time-consuming nature of VOI analysis, which is dependent on the expertise of the person analyzing the data and for which an automated volume measurement technique is lacking. The recently developed automated method of voxel-based morphometry (VBM) (*16*) objectively maps a loss of gray matter on a voxel-by-voxel basis after anatomic standardization analogous to that used in functional neuroimaging. The advantage of VBM over analyses based on VOI is that VBM produces unbiased results from exploration of the whole brain. This approach has been reported to show a higher accuracy for discriminating patients with AD from control subjects than has VOI-based analyses (*17*). A software program that uses VBM for the automated diagnosis of very early AD has been proposed (Figs. 1 and 2) (*18*).

For VBM, a 3-dimensional volumetric acquisition of a T1-weighted gradient-echo sequence produces a gapless series of thin sections with a thickness of approximately

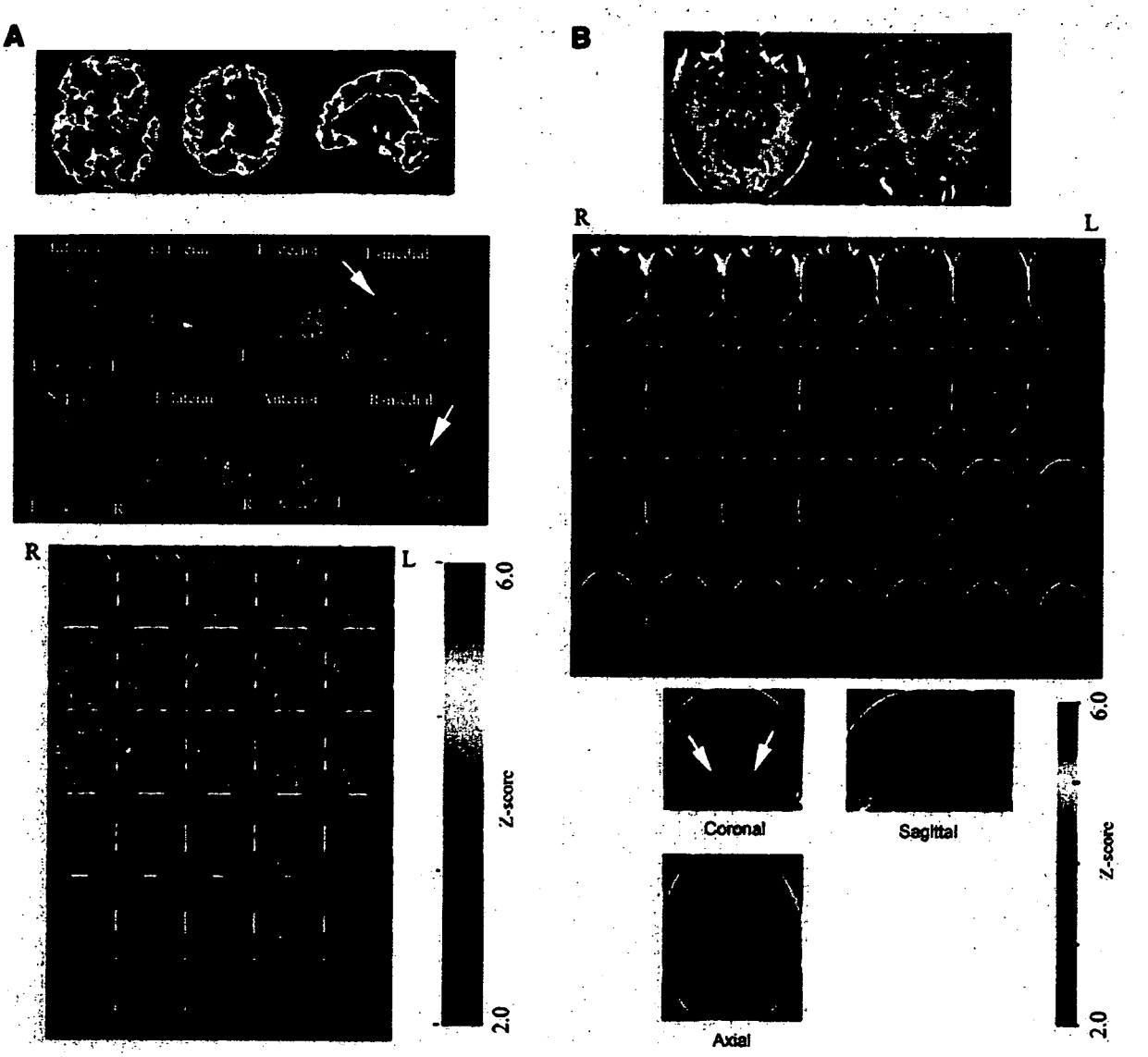

FIGURE 2. Statistical image analysis for 78-y-old woman with amnestic MCI. (A) Brain perfusion SPECT data were analyzed with *z* score mapping system. Specific VOI for very early AD (bilateral posterior cingulate gyri and precunei and parietal association cortex) is demarcated by red lines on MRI template. Significantly decreased rCBF above *z* score of 2 was observed within this specific VOI (arrows). (B) Gray matter images extracted from MR images were analyzed with *z* score mapping system. Specific VOI for very early AD (bilateral medial temporal areas, including parahippocampal gyri and amygdaloid bodies) is demarcated by pink sections on MRI template. Significantly decreased gray matter concentration above *z* score of 2 was observed within this specific VOI (arrows).

1 mm. The original method for VBM included 3 processes: anatomic standardization, segmentation, and smoothing. Images were analyzed with SPM. Anatomic standardization with an affine and nonlinear transformation fits each brain to a standard template brain in 3-dimensional space, so as to correct for differences in brain size and shape and to facilitate intersubject averaging. Anatomically standardized MR images are then segmented into gray matter, white matter, cerebrospinal fluid, and other compartments with a modified version of the clustering algorithm, the maximum-likelihood "mixture model" algorithm. The segmentation procedure involves calculating a Bayesian probability for each voxel to determine whether it belongs to a tissue class on the basis of a priori MRI information with nonuniformity correction. Finally, the gray matter images are smoothed by convolving with an isotropic gaussian kernel to use the partial-volume effect to create a spectrum of gray matter intensities. The gray matter intensities are equivalent to the weighted average of gray matter voxels located in the volume fixed by the smoothing kernel. Regional intensities can therefore be taken as equivalent to gray matter concentrations (*16*).

PARTIAL-VOLUME CORRECTION (PVC)

The more limited spatial resolution of PET and SPECT scanners than of MRI scanners does not allow an exact measurement of the local radiotracer concentration in brain tissue because partial-volume effects cause an underestimation of activity in small structures of the brain. Because brain atrophy accentuates partial-volume effects on PET and SPECT measurements, actual glucose metabolism and rCBF could be underestimated in AD. Therefore, it has been uncertain whether the reductions in glucose metabolism and rCBF observed in AD patients reflect actual reductions or partial-volume effects.

Recent advances in image analysis have made PVC on PET and SPECT images possible with 3 dimensional volumetric T1-weighted MR images. There are 2 MRI-based approaches to PVC. The 2-compartment method (*19*) corrects PET or SPECT data for the diluting effects of cerebrospinal fluid spaces. The 3-compartment method (*20–22*) accounts for the effects of partial-volume averaging between gray matter and white matter. In a comparative study of these 2 methods, Meltzer et al. (*23*) reported greater accuracy for the absolute quantitative measures of the 3-compartment algorithm than for the 2-compartment algorithm. Two-compartment PVC has been reported to be inadequate for the complete recovery of PET or SPECT counts (*23*). However, the 3-compartment algorithm is more sensitive to errors, particularly image segmentation and image registration, and could give rise to approximately 17% error. In the 3-compartment method, PVC is performed by dividing a gray matter PET or SPECT image by a gray matter MR image that has been segmented from an original MR image and further convoluted with spatial resolution equivalent to that of PET or SPECT on a voxel-by-voxel basis. PET or SPECT data reflect both brain volume losses and functional changes. PVC provides a more accurate determination of the regional pattern of rCBF or glucose metabolism in AD by diminishing the artifactual effects of regional differences in tissue loss on the rCBF or glucose metabolism data.

NORMAL AGING AND SEX DIFFERENCES

The prevalence of AD is below 1% in people aged 60–64 y but shows an almost exponential increase with age, so that in people aged 85 y or older, the prevalence is between 24% and 33% in Western countries (*24*). Thus, aging is the most obvious risk factor for AD. Moreover, the female-to-male prevalence of AD is 70% and is likely related to the increased life expectancy of women.

In order to clarify whether AD represents a disease rather than exaggerated aging, the relationship between normal aging and neuroimaging findings should be investigated. Sex differences in neuroimaging findings should also be investigated for the construction of a normal database for statistical image analysis. Hanyu et al. (*25*) reported some sex differences in rCBF patterns in AD patients; men had a more severe decrease in rCBF in the parietal and posterior cingulate cortices, whereas women had a more severe decrease in rCBF in the medial temporal region and frontal lobe.

Numerous investigations on the relationship between advancing age and rCBF or glucose metabolism have been performed. Recent investigations introduced voxel-based analysis in the stereotactic space. In PET studies, the reductions most common with advancing age were observed in the dorsolateral and medial frontal areas and the perisylvian and insular cortices (*26*). Similar results were obtained in recent SPECT studies. Van Laere (*27*) reported an age-related decline in rCBF in the anterior cingulate gyrus, bilateral basal ganglia, and left prefrontal, left lateral frontal, left superior temporal, and insular cortices.

In contrast to the many investigations on the effects of aging, there have been few reports on the relationship between age and rCBF or glucose metabolism after PVC. This situation may be attributable to methodologic difficulties and the necessity for the acquisition of 3-dimensional MR images for PVC. Consistent negative correlations between age and rCBF were observed in the bilateral perisylvian and frontal areas before and after PVC in a SPECT study (*22*). These decreases were independent of differences in global cerebral blood flow between subjects and therefore represented a true age-related redistribution of rCBF. These data suggest a potential true decline in rCBF in these regions with advancing age. On the other hand, Yanase et al. (*28*) reported that PVC largely resolved negative correlations between age and glucose metabolism in the bilateral perisylvian and medial frontal areas before PVC. These data suggest that an apparent decline in glucose metabolism with advancing age is attributable to regional atrophy.

In contrast to negative correlations, positive correlations between age and rCBF showed marked differences before and after PVC in the SPECT study mentioned earlier (*22*). Instead of the positive correlation in the limbic areas before PVC, the sensorimotor and parietal areas showed positive correlations after PVC. This change could be explained by the relationship between age and gray matter volume. The perisylvian and sensorimotor areas showed significant atrophy with advancing age, but the limbic areas showed significant preservation of regional gray matter volume in older subjects. Less influence of PVC in the limbic areas in older subjects would lead to a relative increase in rCBF with advancing age. Good et al. (*29*) studied the effects of aging in 465 normal adult human brains by using the VBM. They observed the relative preservation of gray matter volume symmetrically in the amygdala, hippocampi, entorhinal cortices, and thalami.

Although several investigators have examined sex differences in healthy volunteers by using PET or SPECT, the findings of these studies have been inconsistent and controversial. Sex differences in rCBF in older healthy volunteers were observed with SPECT after PVC (*30*). Women had higher rCBF in the left inferior frontal gyrus, bilateral middle temporal gyri, and left superior temporal gyrus.

Men had higher rCBF in the left superior frontal gyrus, right superior parietal lobule, right postcentral gyrus, right cerebellum, right middle frontal gyrus, right fusiform gyrus, and right precuneus. Sex differences in resting rCBF in the parietal lobes have been reported by other researchers using SPECT. Van Laere et al. (*27*) reported that women had higher rCBF in the right parietal lobe and bilateral parietal lobes than did men.

EARLY DIAGNOSIS OF AD BY NEUROIMAGING

The significance of memory complaints in subjects who do not yet match the criteria for AD but who are at high risk of developing a full-blown dementia syndrome in the next few years has recently attracted attention. This at-risk state is commonly referred to as mild cognitive impairment (MCI) (*31*). It has been recognized that the concept of MCI may be heterogeneous, although the most common subtype, that is, amnestic MCI, likely progresses to AD and fulfills the following criteria: memory concern, usually by the patient but preferably corroborated by an informant; objective memory impairment for age; essentially normal general cognitive function, as judged by a physician; ability to perform normal activities of daily living, as judged by a physician; and not demented.

Cerebral Association Cortex

Many researchers have demonstrated metabolic and blood flow reductions in the parietotemporal association cortex (*32*). This finding has been widely recognized as a diagnostic pattern for AD. The parietotemporal involvement is bilateral, although asymmetry in the degree of perfusion or metabolic reduction is recognized. Thus, it has been reported consistently that the posterior association cortex is the first cortical region to be affected in AD. The deficit spreads to the frontal lobes as the disease progresses, with persisting asymmetry. It has been reported that AD patients with early-onset disease have greater posterior association cortex involvement than patients with late-onset disease (*33*). On the other hand, the primary motor, sensory, and visual cortices are typically spared until the very severe stages of AD (*32*).

Posterior Cingulate Gyrus and Precuneus

In amnestic MCI, a decrease in rCBF as well as glucose metabolism in the posterior cingulate gyrus and precuneus has been observed with PET or SPECT (Fig. 2) (*34,35*). Statistical image analysis with 3D-SSP or SPM has allowed these observations. It is difficult to distinguish a slight decrease in rCBF or metabolism in these areas in patients with early AD by visual inspection because metabolic activity or rCBF in the posterior cingulate gyrus is as high as that in the primary visual cortex in healthy individuals at rest (*34*). A decrease in rCBF in the posterior cingulate gyrus and precuneus of patients with mild AD but without any loss of gray matter volume has been observed (*36*). Reductions in PET measures of glucose metabolism and brain perfusion SPECT measures in AD remain even after accounting for PVC; therefore, these reductions are more than just an artifact resulting from an increase in cerebral fluid space (*13,37*). The superiority of 3D-SSP analysis over visual inspection for discriminating patients with very early AD from control subjects by brain perfusion SPECT has been reported (*38*). In that report, z scores in the posterior cingulate gyrus and precuneus provided a higher accuracy (86%) for discriminating patients with AD from control subjects than did those in the medial temporal areas, parietal association cortices, or temporal association cortices.

The observation that a reduction in metabolism in these areas predicts a cognitive decline in presymptomatic people indicates that the pathophysiologic process begins well before even mild or questionable dementia is recognized clinically (*39*). PET measures of glucose hypometabolism reflect decreased synaptic activity attributable to either a loss or a dysfunction of synapses, and regional metabolic deficits observed on PET may reflect projections from dysfunctional neurons in other brain lesions. In nonhuman primates, lesions of the entorhinal cortex, which is the first region to be affected by AD (*40*), cause a significant and long-lasting metabolic decline in a small set of remote brain regions, especially the inferior parietal, posterior temporal, posterior cingulate, and occipital association cortices and the posterior hippocampal regions (*41*). Mosconi et al. (*42*) and Hirao et al. (*43*) reported functional connectivity between the entorhinal cortex and the posterior cingulate gyrus in AD patients by using ^{18}F-FDG PET and brain perfusion SPECT, respectively. These results suggest that a reduction in rCBF or metabolism in the posterior cingulate gyrus and precuneus indicates that the earliest functional change in AD is a remote effect. Contrary to this hypothesis of a remote effect, some investigators have suggested the presence of pathologic changes in the posterior cingulate gyrus by using VBM to demonstrate localized atrophy in amnestic MCI (*44*).

According to a longitudinal SPECT study (*35*), decreases in the rCBF adjusted for relative flow distribution by normalization of global cerebral blood flow in the posterior cingulate gyrus and precuneus became ambiguous as the disease progressed. This finding may be attributable to a greater stability of relative rCBF in these areas than in other cortical areas in the disease process. This stability was also demonstrated by Tonini et al. (*45*). They reported significant clusters of relative rCBF decreases by using SPM—not in the posterior cingulate gyrus but in the medial part of the temporal lobe in both hemispheres, in the orbital part of the right frontal lobe, and in the inferior part of the right parietal lobe—in a short-term longitudinal evaluation (3 and 6 mo) of mild AD.

The region of the posterior cingulate gyrus and precuneus is known to be important in memory (*46*). The retrosplenial cingulate cortex receives input from the subiculum and projects to the anterior thalamus, thus providing an alternative route between the hippocampus and the thalamus.

This thalamocortical portion of the Papez circuit (entorhinal cortex–hippocampus–mamillary body–anteromedial thalamus–posterior cingulate cortex–entorhinal cortex) (*47*) may be important in memory, with lesions of the retrosplenial cingulate cortex likely causing memory dysfunction by disrupting this pathway.

The PET study of Desgranges et al. also showed activation in the precuneus during an episodic memory retrieval task but not in a control or semantic memory task (*46*). Little is known concerning either the functions or the connectivity of the precuneus. Anatomic evidence indicates prefrontal, temporal, occipital, and thalamic connections to the precuneus.

Medial Temporal Areas

There has been controversy as to whether glucose metabolism or rCBF in the medial temporal areas is decreased or not at an early stage of AD. In a SPECT study (*21*) of patients with mild AD, a significant decrease in absolute rCBF in the amygdala and hippocampus became normal after PVC with a 3-compartment model. These areas have been reported to show marked atrophy from the early stage of AD on (*48*). Therefore, partial-volume effects would mostly affect these areas on SPECT images. Previous studies of brain perfusion SPECT have reported low rCBF in the hippocampus of patients with probable AD (*49*). However, most recent investigations with PET scanners with better spatial resolution have not reported such a decrease in the hippocampus (*50*). These observations suggest that the decrease in rCBF in the hippocampus may be attributable mainly to partial-volume effects on SPECT images. The rCBF per unit volume may be maintained in the medial temporal areas in patients with mild to moderate AD. This maintenance may result from a neuroplastic response in AD. PET measures of glucose metabolism in the entorhinal cortex were most accurate in differentiating subjects with MCI from subjects without MCI (*51*). The selective decrease in rCBF in the parahippocampal regions may be attributable not to incomplete PVC but rather to a hindrance of the disclosure of accurate pathophysiology by the limitation of the spatial resolution of SPECT (*21*).

In contrast to most metabolic neuroimaging studies demonstrating absent hippocampal dysfunction in early AD through voxel-based analysis, some investigators have reported evidence for reduced glucose metabolism in the hippocampus by using an MRI-based region-of-interest technique. Mosconi et al. (*52*) attributed absent hippocampal hypometabolism to inaccurate anatomic standardization in a voxel-based analysis. They observed a significant 14% decrease in absolute glucose metabolism and a significant 18% decrease in volume in the hippocampus of people with MCI relative to healthy control subjects. The use of 2-compartment PVC still resulted in a significant decrease in glucose metabolism in the hippocampus. It is possible that VBM could fail to detect functional abnormalities in relatively small structures, such as the hippocampus, because of failed spatial alignment. Further studies with high-resolution PET (*53*), with less influence of partial-volume effects, may be necessary for this controversy to be settled.

Numerous structural MRI studies have demonstrated that atrophy of the medial temporal lobe, including the hippocampus and the entorhinal cortex, is a sensitive marker of very early AD (Fig. 2). Of the medial temporal lobe structures, it has been argued that a decreased entorhinal cortex volume may be a particularly sensitive predictor of AD on the basis of tangle deposition in the entorhinal cortex during early AD, with subsequent spread to the hippocampus itself (*54*).

Neuropathologic studies have also provided detailed information about which specific brain regions are selectively affected in the earliest stage of AD. The initial neuronal lesions of neurofibrillary tangles and neuritic plaques appear to occur in the entorhinal cortex, a portion of the anterior parahippocampal gyrus that receives projections from widespread limbic and association areas and gives rise to the perforant pathway, the major cortical excitatory input to the hippocampus itself (*40*). Some layers of the entorhinal cortex undergo 40%–60% neuronal depopulation even in the earliest phase of AD (*40*), when memory impairments and patient complaints are subtle and the symptoms do not reach the threshold for the diagnosis of AD. Chetelat et al. (*44*) reported significant losses of gray matter predominantly affecting the hippocampal region and cingulate gyri in patients with amnestic MCI by using VBM. The results were in good agreement with the pathologic changes in the amnestic stage of AD. The VBM study of Hirata et al. (*18*) revealed losses of gray matter selectively in the bilateral medial temporal areas, including the entorhinal areas, in very early AD. In that report, receiver operating characteristic curves for z scores in the bilateral medial temporal areas, including the entorhinal cortex, showed a high accuracy (87.8%) for discriminating patients with very early AD at the MCI stage from normal control subjects. These findings suggest the possibility of using VBM for the early diagnosis of AD. However, care must be taken in this diagnosis. Ishii et al. (*55*) remarked on differences in VBM results between early-onset AD and late-onset AD. Both AD groups had significantly reduced gray matter in the bilateral medial temporal regions. In addition, the early-onset group had more severe losses of gray matter in the parietal cortex, posterior cingulate gyrus, and precuneus.

PREDICTION OF CONVERSION FROM MCI TO AD

When neuropsychological test performance has been used to define MCI, 12%–15% of patients have been shown to have converted to dementia per annum; this incidence is about 10 times higher than the incidence of dementia in the general population (*56*). People with MCI comprise a heterogeneous group of individuals who have a variety of clinical outcomes and who are at risk for developing AD. Prediction of the conversion from MCI to AD on the basis

of initial neuroimaging studies is an important research topic. A recent longitudinal ^{18}F-FDG PET study reported a high predictive value of reduced uptake in the parietal association areas and a lower predictive value of reduced uptake in the posterior cingulate gyrus (*57*). Mosconi et al. (*58*) also reported that, relative to nonconverters, converters (from MCI to AD) demonstrated reduced glucose metabolism in the inferior parietal cortex. These results strongly demonstrate the high predictive value of functional abnormalities in the parietal association areas. In contrast, a longitudinal study (*59*) suggested a high predictive value of functional abnormalities in the posterior cingulate gyrus. A combination of ^{18}F-FDG PET findings and the presence of apolipoprotein E allele ε4 elevated this predictive value (*60*).

Using brain perfusion SPECT to compare 52 converters (from MCI to AD) and 24 nonconverters at a 3-y follow-up, Hirao et al. reported reductions in rCBF in the bilateral parietal areas and the precunei in converters relative to nonconverters (Fig. 3) (*61*). The logistic regression model revealed that a reduction in rCBF in the inferior parietal lobule, angular gyrus, and precuneus had high predictive value and discriminative ability for converters and nonconverters. The data suggest that initial SPECT studies of rCBF in individuals with MCI may be useful in predicting who will convert to AD in the near future. A similar report at a 2-y follow-up in a SPECT study demonstrated that converters showed reduced rCBF specifically in the parietal and temporal lobes, precuneus, and posterior cingulate cortex (*62*).

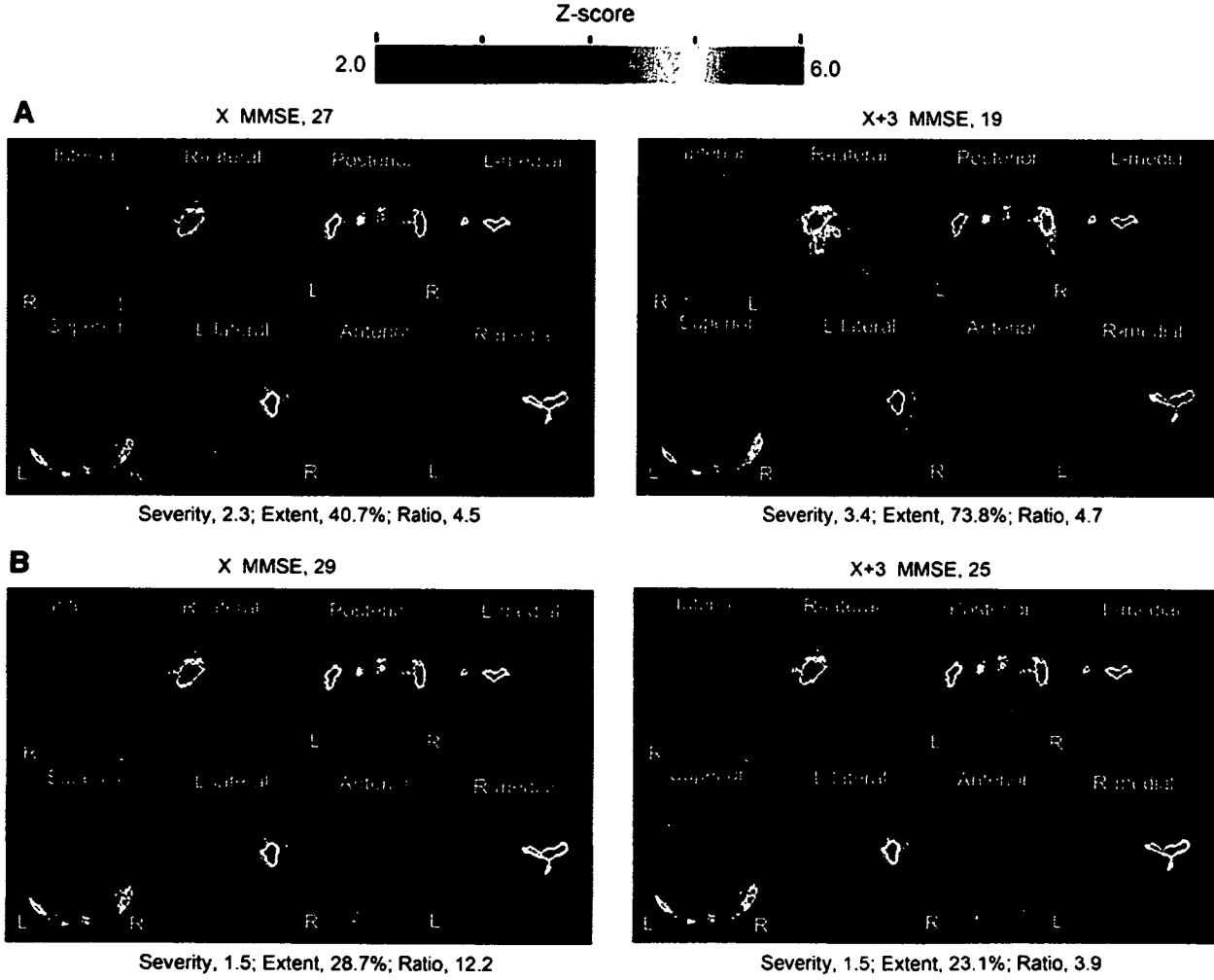

FIGURE 3. Comparison of *z* score mapping results for brain perfusion SPECT for converters (from amnestic MCI to AD) and nonconverters over 3 y. (A) For 56-y-old woman who converted from MCI to AD, high values characterizing decreases in rCBF (severity and extent) were seen even at baseline. These values were markedly elevated 3 y later. (B) For 68-y-old man who did not convert from MCI to AD, low values for severity and extent were seen at baseline. These values were not elevated 3 y later. X MMSE = mean score on Mini-Mental State Examination (MMSE) at the initial study; X+3 MMSE = score on MMSE at 3 y.

Killiany et al. (*63*) used MRI to measure the volumes of the entorhinal cortex and the hippocampus in 137 individuals and found that the volume of the entorhinal cortex distinguished the subjects who were destined to develop dementia with considerable accuracy, whereas the hippocampus measure did not. deToledo-Morrell et al. (*64*) reported that the right hemisphere entorhinal cortex volume was the best predictor of the conversion from MCI to AD, with a concordance rate of 93.5%. Chetelat et al. (*65*) reported significantly greater losses of gray matter in the hippocampal area, inferior and middle temporal gyri, posterior cingulate gyrus, and precuneus in converters (from MCI to AD) than in nonconverters. This accelerated atrophy may result from both neurofibrillary tangle accumulation and parallel pathologic processes, such as functional alterations in the posterior cingulate gyrus.

DIFFERENTIAL DIAGNOSIS OF AD AND OTHER TYPES OF DEMENTIA

Dementia with Lewy Bodies (DLB)

DLB is the second most common form of degenerative dementia, accounting for up to 20% of cases in older people in Europe and the United States. It has also been increasingly diagnosed in Japan in parallel with the development of neuroimaging techniques. It is characterized by the clinical triad of fluctuating cognitive impairment, spontaneous parkinsonism, and recurrent visual hallucinations. Consensus clinical criteria have been published (*66*) and have been shown to have high specificity but may still lack sensitivity. Pathologically, DLB may be classified as a Lewy body disorder or as α-synucleinopathy. Although both DLB and AD show reductions in presynaptic cholinergic transmission from the basal forebrain, in DLB there are also deficits in cholinergic transmission from brain stem nuclei. Postsynaptic cortical muscarinic receptors are more functionally intact in DLB, suggesting a potential responsiveness to cholinergic enhancement. An accurate diagnosis of DLB is clinically important, as the management of psychosis and behavioral disturbances is complicated by sensitivity to neuroleptic medications. There is accumulating evidence to suggest that DLB may be particularly amenable to cholinergic enhancers.

Neuroimaging findings indicated a relative preservation of medial temporal lobe structures and rCBF in DLB (*67, 68*). Significant reductions in dopamine transporter levels were found in the caudate and putamen in subjects with DLB relative to subjects with AD (*69*). Several studies also indicated subtle differences in perfusion patterns on SPECT or ^{18}F-FDG PET, with a greater degree of occipital hypoperfusion or hypometabolism in DLB than in AD (Fig. 4) (*70,71*). Minoshima et al. (*70*) reported a high sensitivity (90%) and a high specificity (80%) for the accuracy of discriminating AD from DLB on the basis of the finding of hypometabolism in the occipital cortex. Recently, an alternative method (cardiac uptake of ^{123}I-metaiodobenzylguanidine) for differentiating AD from DLB was reported (*72*).

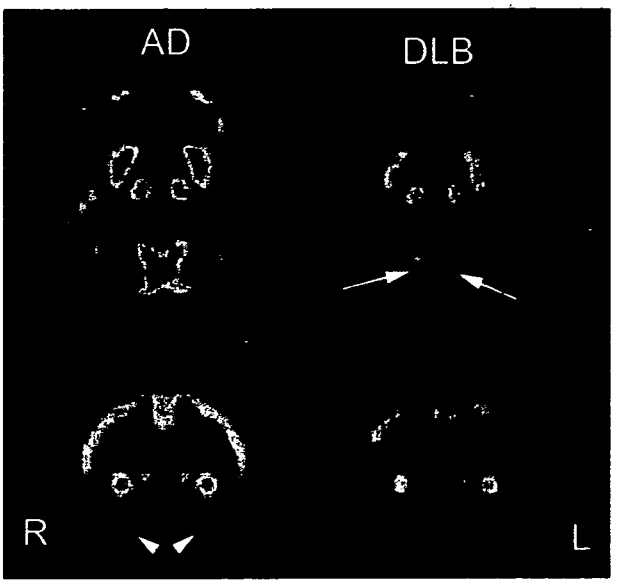

FIGURE 4. Comparison of brain perfusion SPECT images for moderate AD and moderate DLB. DLB showed lower perfusion in occipital cortex than AD (arrows). In contrast, AD showed lower perfusion in medial temporal areas (arrowheads).

Markedly decreased cardiac uptake was observed in DLB because of cardiac sympathetic denervation.

Frontotemporal Dementia (FTD)

FTD is a heterogeneous clinicopathologic syndrome caused by progressive degeneration of the frontal lobes, anterior temporal lobes, or both. In contrast to other types of dementia, FTD involves the relative preservation of memory and visuospatial skills but early alterations in behavior and personality. In the absence of a biologic marker for this disorder, clinicians diagnose FTD on the basis of these criteria and use neuroimaging and other test results as corroborative features. PET and SPECT studies revealed the preferential involvement of the frontotemporal regions in FTD. Jeong et al. (*73*) demonstrated a decrease in glucose metabolism in extensive cortical regions, such as the frontal and anterior temporal areas, cingulate gyri, uncus, and insula, and subcortical areas, including the basal ganglia and medial thalamic regions; this metabolic feature may help to differentiate FTD from AD or other causes of dementia. Bonte et al. (*74*) emphasized the presence of a decrease in rCBF in the posterior cingulate gyrus (posterior cingulate sign) for differentiating AD from FTD. Sixteen of 20 AD patients showed the posterior cingulate sign. In contrast, only 1 of 20 FTD patients showed this sign.

EFFECTS OF CHOLINESTERASE INHIBITORS ON CEREBRAL BLOOD FLOW

In addition to the cortical changes that occur in AD, subcortical neuronal losses occur in the nucleus basalis of Meynert, resulting in decreases in the cortical levels of cholinergic markers (*75*). Pharmacologic, biochemical, and

functional imaging observations have implicated a cholinergic defect underlying many behavioral abnormalities in AD. Donepezil hydrochloride is a piperidine-based acetylcholinesterase inhibitor that is clinically used for the symptomatic treatment of mild to moderate AD. Donepezil has been shown to significantly improve cognition and to maintain global function compared with placebo and also to be well tolerated. The results of 24-wk studies have indicated that the well-established benefits of donepezil for cognition may extend to an improvement in the ability to perform complex activities of daily living (*76*). Although donepezil has been approved in many countries for the treatment of mild to moderate AD, its effect on cerebral blood flow or metabolism has not been fully investigated yet.

Using ^{99m}Tc-hexamethylpropyleneamine oxime SPECT with SPM analysis, Mega et al. (*77*) found that the presence of lower lateral orbital frontal and dorsolateral frontal

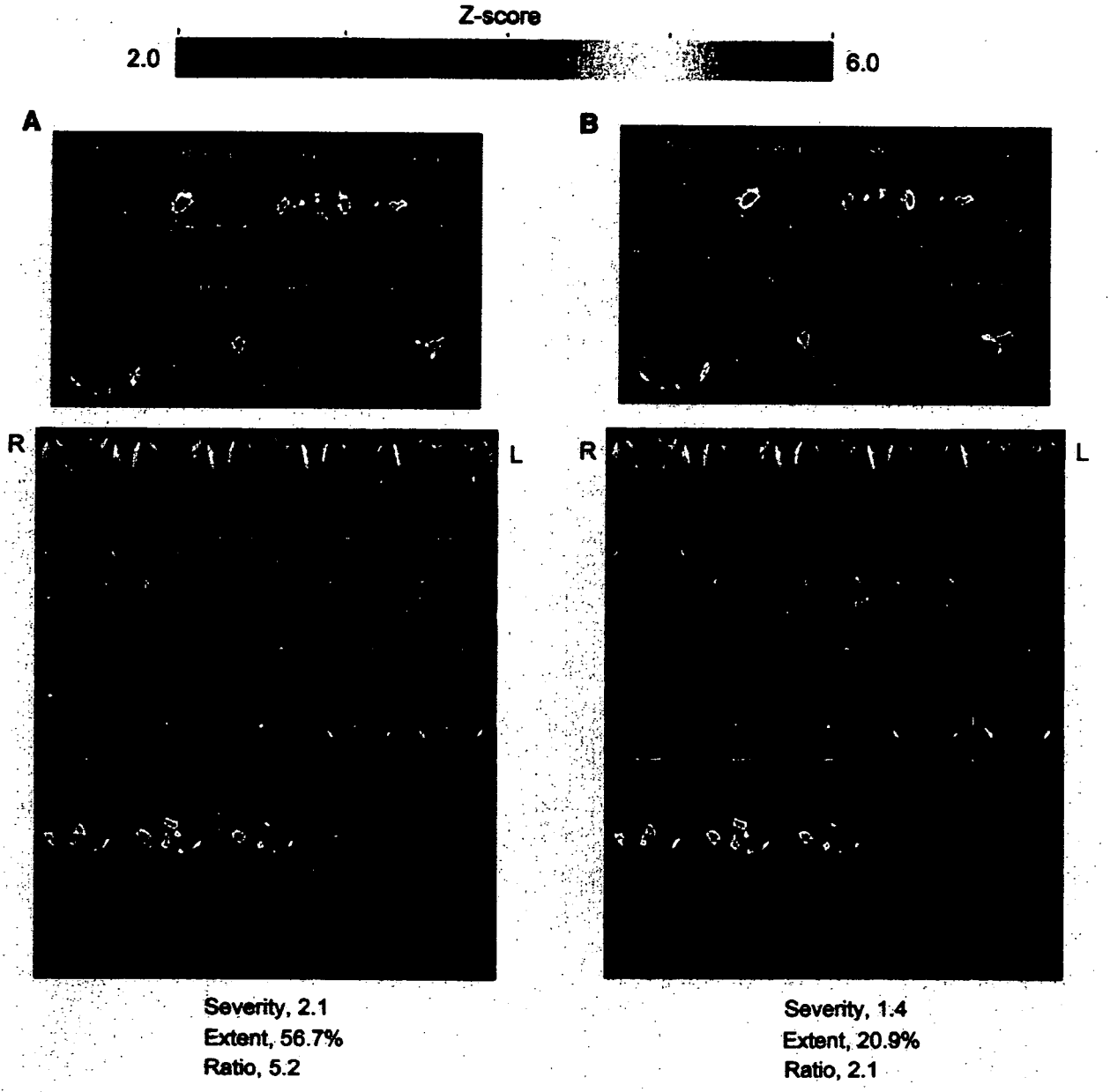

FIGURE 5. Evaluation with *z* score mapping system of therapeutic effects of donepezil on brain perfusion SPECT for 68-y-old woman. (A) Baseline study 1 mo before donepezil showed significant decrease in rCBF within specific VOI for early AD. Mini-Mental State Examination (MMSE) score was 5 (out of 30). (B) At 3 mo after start of donepezil administration, all rCBF indices decreased from values at initial study, indicating amelioration of rCBF within specific VOI. MMSE score increased to 14 (out of 30).

perfusion suggested a good response to donepezil and was significantly related to behaviors of irritability, disinhibition, and euphoria. Nobili et al. (*78*) compared the longitudinal SPECT findings over 15 mo, on average, between stabilized and nonstabilized subjects receiving donepezil treatment. No significant difference was found between the baseline and repeat SPECT data in the stabilized subjects. In contrast, in the nonstabilized subjects, a significant reduction in rCBF was found in the frontal, temporal, and parietal superficial cortices and in the occipital precuneus in the right hemisphere and in the frontal and mesial temporal cortices in the left hemisphere. On repeat SPECT, rCBF was found to be significantly lower in the left frontal region in the nonstabilized subjects than in the stabilized subjects. Ceravolo et al. (*79*) reported that SPM analysis revealed significant increases in rCBF in the right anterior cingulate, dorsolateral prefrontal, and bilateral temporoparietal areas after short-term (4-mo) acetylcholinesterase inhibitor therapy with respect to the baseline. These data suggest that cognitive or behavioral benefits after cholinesterase inhibitor therapy are related to clear increases in rCBF in crucial areas specifically involved in the attention and limbic networks. The longitudinal study of Nakano et al. (*80*) showed that, before and 1 y after the administration of donepezil, the adjusted rCBF was significantly preserved in the right and left anterior cingulate gyri, right middle temporal gyrus, right inferior parietal lobule, and prefrontal cortex in 15 donepezil-treated AD patients compared with 20 placebo-treated AD patients. Treatment with donepezil appeared to reduce the decline in rCBF, suggesting a preservation of functional brain activity (Fig. 5).

CONCLUSION

PET, SPECT, and MRI have played very important roles in diagnosing early AD at the MCI stage, staging AD, differentiating AD from other types of dementia, predicting the conversion from MCI to AD, and assessing therapeutic indications and their effects. A recent advance in voxel-based statistical analysis of PET, SPECT, and MRI data has markedly enhanced the value of neuroimaging in the analysis of dementia.

REFERENCES

1. Terry RD, Masliah E, Salmon DP, et al. Physical basis of cognitive alterations in Alzheimer's disease: synapse loss is the major correlate of cognitive impairment. *Ann Neurol.* 1991;30:572–580.
2. Wallin AK, Andreasen N, Eriksson S, et al. Donepezil in Alzheimer's disease: what to expect after 3 years of treatment in a routine clinical setting. *Dement Geriatr Cogn Disord.* 2007;23:150–160.
3. Winblad B, Wimo A, Engedal K, et al. 3-Year study of donepezil therapy in Alzheimer's disease: effects of early and continuous therapy. *Dement Geriatr Cogn Disord.* 2006;21:353–363.
4. Zamrini E, De Santi S, Tolar M. Imaging is superior to cognitive testing for early diagnosis of Alzheimer's disease. *Neurobiol Aging.* 2004;25:685–691.
5. Silverman DH, Gambhir SS, Huang HW, et al. Evaluating early dementia with and without assessment of regional cerebral metabolism by PET: a comparison of predicted costs and benefits. *J Nucl Med.* 2002;43:253–266.
6. Silverman DH. Brain ^{18}F-FDG PET in the diagnosis of neurodegenerative dementias: comparison with perfusion SPECT and with clinical evaluations lacking nuclear imaging. *J Nucl Med.* 2004;45:594–607.
7. Messa C, Perani D, Lucignani G, et al. High-resolution technetium-99m-HMPAO SPECT in patients with probable Alzheimer's disease: comparison with fluorine-18-FDG PET. *J Nucl Med.* 1994;35:210–216.
8. Herholz K, Schopphoff H, Schmidt M, et al. Direct comparison of spatially normalized PET and SPECT scans in Alzheimer's disease. *J Nucl Med.* 2002; 43:21–26.
9. Bradley KM, O'Sullivan VT, Soper ND, et al. Cerebral perfusion SPET correlated with Braak pathological stage in Alzheimer's disease. *Brain.* 2002; 125:1772–1781.
10. Frith CD, Friston KJ, Ashburner J, et al. Principles and methods. In: Frackowiak RSJ, Friston KJ, Frith CD, Dolan RJ, Mazziotta JC, eds. *Human Brain Function.* San Diego, CA: Academic Press; 1997:3–159.
11. Minoshima S, Frey KA, Koeppe RA, Foster NL, Kuhl DE. A diagnostic approach in Alzheimer's disease using three-dimensional stereotactic surface projections of fluorine-18-FDG PET. *J Nucl Med.* 1995;36:1238–1248.
12. Matsuda H, Mizumura S, Soma T, Takemura N. Conversion of brain SPECT images between different collimators and reconstruction processes for analysis using statistical parametric mapping. *Nucl Med Commun.* 2004;25:67–74.
13. Kanetaka H, Matsuda H, Asada T, et al. Effects of partial volume correction on discrimination between very early Alzheimer's dementia and controls using brain perfusion SPECT. *Eur J Nucl Med Mol Imaging.* 2004;31:975–980.
14. Matsuda H, Mizumura S, Nagao T, et al. Automated discrimination between very early Alzheimer disease and controls using an easy Z-score imaging system for multicenter brain perfusion single-photon emission tomography. *AJNR.* 2007;28: 731–736.
15. Ishii K, Willoch F, Minoshima S, et al. Statistical brain mapping of ^{18}F-FDG PET in Alzheimer's disease: validation of anatomic standardization for atrophied brains. *J Nucl Med.* 2001;42:548–557.
16. Ashburner J, Friston KJ. Voxel-based morphometry: the methods. *Neuroimage.* 2000;11:805–821.
17. Testa C, Laakso MP, Sabattoli F, et al. A comparison between the accuracy of voxel-based morphometry and hippocampal volumetry in Alzheimer's disease. *J Magn Reson Imaging.* 2004;19:274–282.
18. Hirata Y, Matsuda H, Nemoto K, et al. Voxel-based morphometry to discriminate early Alzheimer's disease from controls. *Neurosci Lett.* 2005;382:269–274.
19. Meltzer CC, Zubieta JK, Brandt J, Tune LE, Mayberg HS, Frost JJ. Regional hypometabolism in Alzheimer's disease as measured by positron emission tomography after correction for effects of partial volume averaging. *Neurology.* 1996;47:454–461.
20. Mueller-Gaertner HW, Links JM, Prince JL, et al. Measurement of radiotracer concentration in brain gray matter using positron emission tomography: MRI-based correction for partial volume effects. *J Cereb Blood Flow Metab.* 1992;12: 571–583.
21. Matsuda H, Kanetaka H, Ohnishi T, et al. Brain SPET abnormalities in Alzheimer's disease before and after atrophy correction. *Eur J Nucl Med Mol Imaging.* 2002;29:1502–1505.
22. Matsuda H, Ohnishi T, Asada T, et al. Correction for partial-volume effects on brain perfusion SPECT in healthy men. *J Nucl Med.* 2003;44:1243–1252.
23. Meltzer CC, Kinahan PE, Greer PJ, et al. Comparative evaluation of MR-based partial-volume correction schemes for PET. *J Nucl Med.* 1999;40:2053–2065.
24. Blennow K, de Leon MJ, Zetterberg H. Alzheimer's disease. *Lancet.* 2006;368: 387–403.
25. Hanyu H, Shimizu S, Tanaka Y, Takasaki M, Koizumi K, Abe K. Differences in regional cerebral blood flow patterns in male versus female patients with Alzheimer disease. *AJNR.* 2004;25:1199–1204.
26. Baron JC, Godeau C. Human aging. In: Toga A, Mazziotta JC, eds. *Brain Mapping: The Systems.* San Diego, CA: Academic Press; 2000;591–604.
27. Van Laere K, Versijpt J, Audenaert K, et al. ^{99m}Tc-ECD brain perfusion SPET: variability, asymmetry and effects of age and gender in healthy adults. *Eur J Nucl Med.* 2001;28:873–887.
28. Yanase D, Matsunari I, Yajima K, et al. Brain FDG PET study of normal aging in Japanese: effect of atrophy correction. *Eur J Nucl Med Mol Imaging.* 2005;32: 794–805.
29. Good CD, Johnsrude IS, Ashburner J, Henson RNA, Friston KJ, Frackowiak RSJ. A voxel-based morphometric study of ageing in 465 normal adult human brains. *Neuroimage.* 2001;14:21–36.
30. Li ZJ, Matsuda H, Asada T, et al. Gender difference in brain perfusion ^{99m}Tc-ECD SPECT in aged healthy volunteers after correction for partial volume effects. *Nucl Med Commun.* 2004;25:999–1005.
31. Petersen RC, Doody R, Kurz A, et al. Current concepts in mild cognitive impairment. *Arch Neurol.* 2001;58:1985–1992.

32. Herholz K, Adams R, Kessler J, Szelies B, Grond M, Heiss WD. Criteria for the diagnosis of Alzheimer's disease with PET. *Dementia.* 1990;1:156–164.
33. Kemp PM, Holmes C, Hoffmann SM, et al. Alzheimer's disease: differences in technetium-99m HMPAO SPECT scan findings between early onset and late onset dementia. *J Neurol Neurosurg Psychiatry.* 2003;74:715–719.
34. Minoshima S, Giordani B, Berent S, et al. Metabolic reduction in the posterior cingulate cortex in very early Alzheimer's disease. *Ann Neurol.* 1997;42:85–94.
35. Kogure D, Matsuda H, Ohnishi T, et al. Longitudinal evaluation of early Alzheimer's disease using brain perfusion SPECT. *J Nucl Med.* 2000;41:1155–1162.
36. Matsuda H, Kitayama N, Ohnishi T, et al. Longitudinal evaluation of both morphologic and functional changes in the same individuals with Alzheimer's disease. *J Nucl Med.* 2002;43:304–311.
37. Ibanez V, Pietrini P, Alexandar GE, et al. Regional glucose metabolic abnormalities are not the result of atrophy in Alzheimer's disease. *Neurology.* 1998;50:1585–1593.
38. Imabayashi E, Matsuda H, Asada T, et al. Superiority of 3-dimensional stereotactic surface projection analysis over visual inspection in discrimination of patients with very early Alzheimer's disease from controls using brain perfusion SPECT. *J Nucl Med.* 2004;45:1450–1457.
39. Small GW, Ercoli LM, Silverman DH, et al. Cerebral metabolic and cognitive decline in persons at genetic risk for Alzheimer's disease. *Proc Natl Acad Sci USA.* 2000;97:6037–6042.
40. Gomez-Isla T, Price TL, McKeel DW, et al. Profound loss of layer II entorhinal cortex neurons occurs in very mild Alzheimer's disease. *J Neurosci.* 1996;16:4491–4500.
41. Meguro K, Blaizot X, Kondoh Y, Le Mestric C, Baron JC, Chavoix C. Neocortical and hippocampal glucose hypometabolism following neurotoxic lesions of the entorhinal and perirhinal cortices in the non-human primate as shown by PET: implications for Alzheimer's disease. *Brain.* 1999;122:1519–1531.
42. Mosconi L, Pupi A, De Cristofaro MT, Fayyaz M, Sorbi S, Herholz K. Functional interactions of the entorhinal cortex: an ^{18}F-FDG PET study on normal aging and Alzheimer's disease. *J Nucl Med.* 2004;45:382–392.
43. Hirao K, Ohnishi T, Matsuda H, et al. Functional interactions between entorhinal cortex and posterior cingulate cortex at the very early stage of Alzheimer's disease using brain perfusion single-photon emission computed tomography. *Nucl Med Commun.* 2006;27:151–156.
44. Chetelat G, Desgranges B, De La Sayette V, Viader F, Eustache F, Baron JC. Mapping gray matter loss with voxel-based morphometry in mild cognitive impairment. *Neuroreport.* 2002;13:1939–1943.
45. Tonini G, Shanks MF, Venneri A. Short-term longitudinal evaluation of cerebral blood flow in mild Alzheimer's disease. *Neurol Sci.* 2003;24:24–30.
46. Desgranges B, Baron JC, de la Sayette V, et al. The neural substrates of memory systems impairment in Alzheimer's disease: a PET study of resting brain glucose utilization. *Brain.* 1998;121:611–631.
47. Papez JW. A proposed mechanism of emotion. *Arch Neurol Psychiatry.* 1937;38:725–743.
48. Baron JC, Chetelat G, Desganges B, et al. In vivo mapping of gray matter loss with voxel-based morphometry in mild Alzheimer's disease. *Neuroimage.* 2001;14:298–309.
49. Ohnishi T, Hoshi H, Nagamachi S, et al. High-resolution SPECT to assess hippocampal perfusion in neuropsychiatric diseases. *J Nucl Med.* 1995;36:1163–1169.
50. Ishii K, Sasaki M, Yamaji S, Sakamoto S, Kitagaki H, Mori E. Paradoxical hippocampus perfusion in mild-to-moderate Alzheimer's disease. *J Nucl Med.* 1998;39:293–298.
51. De Santi S, de Leon MJ, Rusinek H, et al. Hippocampal formation glucose metabolism and volume losses in MCI and AD. *Neurobiol Aging.* 2001;22:529–539.
52. Mosconi L, Tsui WH, De Santi S, et al. Reduced hippocampal metabolism in MCI and AD: automated FDG-PET image analysis. *Neurology.* 2005;64:1860–1867.
53. Valk PE, Jagust WJ, Derenzo SE, Huesman RH, Geyer AB, Budinger TF. Clinical evaluation of a high-resolution (2.6-mm) positron emission tomography. *Radiology.* 1990;176:783–790.
54. Du AT, Schuff N, Amend D, et al. Magnetic resonance imaging of the entorhinal cortex and hippocampus in mild cognitive impairment and Alzheimer's disease. *J Neurol Neurosurg Psychiatry.* 2001;71:441–447.
55. Ishii K, Kawachi T, Sasaki H, et al. Voxel-based morphometric comparison between early- and late-onset mild Alzheimer's disease and assessment of diagnostic performance of z score images. *AJNR.* 2005;26:333–340.
56. Celsis P. Age-related cognitive decline, mild cognitive impairment or preclinical Alzheimer's disease? *Ann Med.* 2000;32:6–14.
57. Chetelat G, Desgranges B, de la Sayette V, Viader F, Eustache F, Baron JC. Mild cognitive impairment: can FDG-PET predict who is to rapidly convert to Alzheimer's disease? *Neurology.* 2003;60:1374–1377.
58. Mosconi L, Perani D, Sorbi S, et al. MCI conversion to dementia and the APOE genotype: a prediction study with FDG-PET. *Neurology.* 2004;63:2332–2340.
59. Drzezga A, Lautenschlager N, Siebner H, et al. Cerebral metabolic changes accompanying conversion of mild cognitive impairment into Alzheimer's disease: a PET follow-up study. *Eur J Nucl Med Mol Imaging.* 2003;30:1104–1113.
60. Drzezga A, Grimmer T, Riemenschneider M. Prediction of individual clinical outcome in MCI by means of genetic assessment and ^{18}F-FDG PET. *J Nucl Med.* 2005;46:1625–1632.
61. Hirao K, Ohnishi T, Hirata Y, et al. The prediction of rapid conversion to Alzheimer's disease in mild cognitive impairment using regional cerebral blood flow SPECT. *Neuroimage.* 2005;28:1014–1021.
62. Borroni B, Anchisi D, Paghera B, et al. Combined ^{99m}Tc-ECD SPECT and neuropsychological studies in MCI for the assessment of conversion to AD. *Neurobiol Aging.* 2006;27:24–31.
63. Killiany RJ, Hyman BT, Gomez-Isla T, et al. MRI measures of entorhinal cortex vs hippocampus in preclinical AD. *Neurology.* 2002;58:1188–1196.
64. deToledo-Morrell L, Stoub TR, Bulgakova M, et al. MRI-derived entorhinal volume is a good predictor of conversion from MCI to AD. *Neurobiol Aging.* 2004;25:1197–1203.
65. Chetelat G, Landeau B, Eustache F, et al. Using voxel-based morphometry to map the structural changes associated with rapid conversion in MCI: a longitudinal MRI study. *Neuroimage.* 2005;27:934–946.
66. McKeith IG, Dickson DW, Lowe J, et al. Diagnosis and management of dementia with Lewy bodies: third report of the DLB Consortium. *Neurology.* 2005;65:1863–1872.
67. Barber R, Ballard C, McKeith IG, Gholkar A, O'Brien JT. MRI volumetric study of dementia with Lewy bodies: a comparison with AD and vascular dementia. *Neurology.* 2000;54:1304–1309.
68. Colloby SJ, Fenwick JD, Williams ED, et al. A comparison of (99m)Tc-HMPAO SPET changes in dementia with Lewy bodies and Alzheimer's disease using statistical parametric mapping. *Eur J Nucl Med Mol Imaging.* 2002;29:615–622.
69. O'Brien JT, Colloby S, Fenwick J, et al. Dopamine transporter loss visualized with FP-CIT SPECT in the differential diagnosis of dementia with Lewy bodies. *Arch Neurol.* 2004;61:919–925.
70. Minoshima S, Foster NL, Sima AA, Frey KA, Albin RL, Kuhl DE. Alzheimer's disease versus dementia with Lewy bodies: cerebral metabolic distinction with autopsy confirmation. *Ann Neurol.* 2001;50:358–365.
71. Pasquier J, Michel BF, Brenot-Rossi I, Hassan-Sebbag N, Sauvan R, Gastaut JL. Value of (99m)Tc-ECD SPET for the diagnosis of dementia with Lewy bodies. *Eur J Nucl Med Mol Imaging.* 2002;29:1342–1348.
72. Yoshita M, Taki J, Yokoyama K, et al. Value of ^{123}I-MIBG radioactivity in the differential diagnosis of DLB from AD. *Neurology.* 2006;66:1850–1854.
73. Jeong Y, Cho SS, Park JM, et al. ^{18}F-FDG PET findings in frontotemporal dementia: an SPM analysis of 29 patients. *J Nucl Med.* 2005;46:233–239.
74. Bonte FJ, Harris TS, Roney CA, Hynan LS. Differential diagnosis between Alzheimer's and frontotemporal disease by the posterior cingulate sign. *J Nucl Med.* 2004;45:771–774.
75. Whitehouse PJ, Price DL, Struble RG, Clark AW, Coyle JT, Delon MR. Alzheimer's disease and senile dementia: loss of neurons in the basal forebrain. *Science.* 1982;215:1237–1239.
76. Rogers SL, Farlow MR, Doody RS, et al. A 24-week, double-blind, placebo-controlled trial of donepezil in patients with Alzheimer's disease. *Neurology.* 1998;50:136–145.
77. Mega MS, Dinov ID, Lee L, et al. Oribital and dorsolateral frontal perfusion defect associated with behavioral response to cholinesterase inhibitor therapy in Alzheimer's disease. *J Neuropsychiatry Clin Neurosci.* 2000;12:209–218.
78. Nobili F, Koulibaly M, Vitali P, et al. Brain perfusion follow-up in Alzheimer's patients during treatment with acetylcholinesterase inhibitors. *J Nucl Med.* 2002;43:983–990.
79. Ceravolo R, Volterrani D, Tognoni G, et al. Cerebral perfusional effects of cholinesterase inhibitors in Alzheimer disease. *Clin Neuropharmacol.* 2004;27:166–170.
80. Nakano S, Asada T, Matsuda H, Uno M, Takasaki M. Donepezil hydrochloride preserves regional cerebral blood flow in patients with Alzheimer's disease. *J Nucl Med.* 2001;42:1441–1445.

ORIGINAL RESEARCH

Automated Discrimination Between Very Early Alzheimer Disease and Controls Using an Easy *Z*-Score Imaging System for Multicenter Brain Perfusion Single-Photon Emission Tomography

H. Matsuda
S. Mizumura
T. Nagao
T. Ota
T. Iizuka
K. Nemoto
N. Takemura
H. Arai
A. Homma

BACKGROUND AND PURPOSE: In Alzheimer disease (AD), a peculiar regional cerebral blood flow (rCBF) abnormality has been reported in the posterior cingulate gyri and precunei, even at a very early stage. We performed a multicenter brain perfusion single-photon emission tomography (SPECT) study to evaluate the discrimination ability of an easy *Z*-score imaging system (eZIS) with a common normal data base between patients with very early AD at the stage of mild cognitive impairment and age-matched healthy controls.

MATERIALS AND METHODS: For a multicenter study, SPECT images of 40 patients with AD and 40 healthy volunteers were acquired from 4 gamma camera systems in 4 different institutions. Systematic differences of SPECT images between gamma cameras were corrected by using conversion maps calculated from the SPECT images of the same brain phantom. Receiver operating characteristic (ROC) analysis was performed to discriminate patients and controls by using a *Z*-score in the volume of interest (VOI), which had been defined as a region related to AD in subjects other than those in a multicenter study.

RESULTS: Bilateral posterior cingulate gyri, precunei, and parietal cortices were defined as a VOI showing rCBF reduction in very early AD. A new indicator of rCBF abnormality in the VOI provided 86% accuracy for distinction of AD and healthy controls in the multicenter study. The area under the ROC curve was 0.934.

CONCLUSION: Because an eZIS can use a common normal data base by converting site-specific SPECT data to the core data, the eZIS was useful for automated diagnosis of very early AD in routine studies in multiple institutions.

In the very early stage of Alzheimer disease (AD), even before a clinical diagnosis of probable AD is possible, decreases in regional cerebral blood flow (rCBF) and glucose metabolism in the posterior cingulate gyri, precunei, and parietal cortices have been reported by using positron-emission tomography (PET)[1,2] or single-photon emission tomography (SPECT).[3,4] We have already reported[5] the superiority of the computer-assisted analysis of SPECT images using 3D stereotactic surface projection (3D-SSP) over visual inspection in the discrimination, from controls, of very early AD at the stage of mild cognitive impairment (MCI).[6] However, this statistical approach requires a control data base for SPECT images. Even if one institution constructs a site-specific normal data base from the same camera and under the same processes for reconstruction of SPECT images, the transfer of this data base to other institutions is hampered by the physical characteristics of the SPECT cameras and collimators used. Despite the fact that the same types of cameras and collimators are used in several institutions, differences in the processes of reconstruction of SPECT images may also give rise to significant variations in the final SPECT images. To make it possible to share a normal data base in SPECT studies, we previously developed a new method using brain phantom experiments.[7] In this method, a 3D conversion map was created from the division of 2 SPECT images of the same phantom obtained from the 2 different cameras after anatomic standardization by statistical parametric mapping (SPM).[8] The conversion map was applied to convert an anatomically standardized SPECT image obtained from one camera to that from the other camera. This conversion algorithm was incorporated in a software program recently developed by us, easy *Z*-score imaging system (eZIS),[9] for statistical analysis of SPECT images. The use of eZIS facilitates sharing of a normal data base of SPECT images in different institutions with different cameras.[10] In the present study, we performed a multicenter SPECT study to evaluate the discrimination ability of eZIS with a common normal data base, between patients with very early AD and age-matched healthy volunteers, collected from different institutions by using different cameras.

Received May 2, 2006; accepted after revision June 14.

From the Department of Nuclear Medicine (H.M.), Saitama Medical University Hospital; the Department of Radiology (H.M., K.N.), National Center Hospital for Mental, Nervous, and Muscular Disorders, National Center of Neurology and Psychiatry; the Department of Radiology (S.M.), Nippon Medical School; the Department of Neurology (T.N.), Tokyo Metropolitan Ebara Hospital; the Department of Psychiatry (T.O., H.A.), Juntendo University School of Medicine; the Department of Nuclear Medicine (T.I.), Fukujuji Hospital; the Department of Neuropsychiatry (K.N.), Institute of Clinical Medicine, University of Tsukuba; Daiichi Radioisotope Laboratory (N.T.); and the Department of Psychiatry (A.H.), Tokyo Metropolitan Institute of Gerontology.

Please address correspondence to Hiroshi Matsuda, MD, Department of Nuclear Medicine, Saitama Medical University Hospital, 38, Morohongo, Moroyama-machi, Iruma-gun, Saitama, 350-0495, Japan; e-mail: matsudah@saitama-med.ac.jp

Materials and Methods

Subjects for Determination of a Specific Region Showing rCBF Reduction in Very Early AD (Group 1)

Sixty healthy controls (28 men and 32 women; 54–83 years of age; mean, 71.5; SD, 8.3) and 29 patients with AD (13 men and 16 women; 57–85 years of age; mean, 70.9; SD, 7.8) at the stage of amnestic type of MCI, who showed progressive cognitive decline and eventually

fulfilled the diagnosis of probable AD according to the National Institute of Neurologic and Communicative Disorders and Stroke and the Alzheimer Disease and Related Disorders Association (NINCDS-ADRDA) criteria[11] during the subsequent follow-up period of 2–6 years, were included in this study. Patients were recruited from those who complained of memory impairment in an outpatient memory clinic of the National Center Hospital for Mental, Nervous, and Muscular Disorders, National Center of Neurology and Psychiatry. At the first visit, they showed selective impairment in delayed recall (>1.5 SD below age-matched normal mean scores of a word-list learning test, a story-recall test, or the Rey-Osterrieth Complex Figure Test) in neuropsychologic examinations without apparent loss in general cognitive, behavioral, or functional status. They corresponded to 0.5 in the Clinical Dementia Rating (CDR).[12] The Mini-Mental State Examination (MMSE)[13] score ranged from 24 to 28 (mean, 25.8 ± 1.5) at the initial visit.

Control subjects were healthy volunteers without memory impairment or cognitive disorders who were recruited from the National Center Hospital for Mental, Nervous, and Muscular Disorders, National Center of Neurology and Psychiatry and whose MMSE scores ranged from 26 to 30 (mean, 28.5 ± 1.4). They did not differ significantly in age or education from the patients with AD.

Subjects for Automated Discrimination Between Very Early AD and Controls in a Multicenter Study (Group 2)

We retrospectively studied different subjects from group 1 comprising 40 patients with AD (15 men and 25 women; 51–83 years of age; mean, 71.0; SD, 8.5) at the stage of amnesic type of MCI, who also showed progressive cognitive decline and eventually fulfilled the diagnosis of probable AD according to NINCDS-ADRDA during the subsequent follow-up period of at least 2 years. They were recruited from patients who complained of memory impairment in an outpatient memory clinic of the Tokyo Metropolitan Ebara Hospital (18 patients); the National Center Hospital for Mental, Nervous, and Muscular Disorders, National Center of Neurology and Psychiatry (14 patients without duplication of patients with AD in group 1); the Juntendo University School of Medicine (7 patients); and the Fukujuji Hospital (1 patient). At the first visit, they showed selective impairment in delayed recall. They also corresponded to 0.5 in CDR. Their MMSE scores ranged from 24 to 28 (mean, 25.7 ± 1.6) at the initial visit.

Forty control subjects (18 men and 22 women; 50–83 years of age; mean, 71.0; SD, 0.3) were healthy volunteers without memory impairment or cognitive disorders. They were recruited from the Tokyo Metropolitan Ebara Hospital (17 subjects) and the National Center Hospital for Mental, Nervous, and Muscular Disorders, National Center of Neurology and Psychiatry (23 subjects without duplication of healthy subjects in group 1). Specifically, their performance was within normal limits (<1 SD) on both the Wechsler Memory Scale-Revised and the Wechsler Adult Intelligence Scale-Revised, and their MMSE score ranged from 26 to 30 (mean, 28.7 ± 1.5).

The local ethics committee approved this study for both healthy volunteers and AD subjects, all of whom gave their informed consent to participate. All subjects were right-handed, screened by a questionnaire regarding medical history, and excluded if they had neurologic, psychiatric, or medical conditions that could potentially affect the central nervous system, such as substance abuse or dependence, atypical headache, head trauma with loss of consciousness, asymptomatic or symptomatic cerebral infarction detected by T2-weighted MR imaging, hypertension, chronic lung disease, kidney disease, chronic hepatic disease, cancer, or diabetes mellitus.

Gamma Cameras

SPECT studies were performed on 4 gamma camera systems in 4 different institutions. The core dataset was acquired in the National Center Hospital for Mental, Nervous, and Muscular Disorders on a Multispect3 triple-headed camera (Siemens Medical Systems, Hoffman Estates, Ill) equipped with low-energy high-resolution fanbeam collimators (camera 1). Camera 2 in the Tokyo Metropolitan Ebara Hospital was a Prism 3000 triple-headed camera (Philips Medical Systems, Andover, Mass) equipped with low-energy high-resolution Fanbeam collimators. Camera 3 in the Juntendo University School of Medicine was a GCA9300A triple-headed camera (Toshiba Medical Systems, Tokyo, Japan) equipped with low-energy high-resolution Fanbeam collimators. Camera 4 in the Fukujuji Hospital was an E-CAM 2-headed camera (Toshiba Medical Systems) equipped with low-energy high-resolution Fanbeam collimators.

Before the SPECT scanning was performed, all subjects had an intravenous line established in all institutions. They were injected while lying down in the supine position with eyes closed in a dimly lit quiet room. Each subject received an intravenous injection of 600–740 MBq of technetium Tc99m ethyl cysteinate dimmer (Tc99m-ECD). Ten minutes after the injection of Tc99m-ECD, brain SPECT was performed. Preprocessing of projection data was performed by using a Hanning filter in camera 1 and a Butterworth filter in the other cameras. Reconstruction was performed by using a Shepp-Logan filter in camera 1 and a ramp filter in other cameras. Scatter correction was performed in cameras 1 and 3, but not in cameras 2 and 4. Attenuation correction was performed in cameras 1 and 2, but not in cameras 3 and 4. To share a normal data base, we performed Hoffman 3D Brain Phantom (Biodex Medical Systems, Shirley, NY) experiments by using these 4 cameras. The phantom was filled with 74 MBq of Tc99m pertechnetate, and SPECT data of the filled phantom were acquired and processed in the same manner as in the human brain study in each institution.

Determination of a Specific Region Showing rCBF Reduction in Very Early AD in Group 1

Voxel-based analysis for comparison of SPECT data of group 1 subjects between 60 controls and 29 patients with very early AD was performed by using Statistical Parametric Mapping 2 (SPM2) (Wellcome Department of Cognitive Neurology, London, UK) running on MATLAB (The MathWorks, Sherborn, Mass). The images were spatially normalized by using SPM2 to an original template for Tc99m-ECD.[14] Then, images were smoothed with a gaussian kernel, 12 mm in full width at half maximum (FWHM). The processed images were analyzed by using SPM2. The effect of global differences in cerebral blood flow between scanning was removed by proportional scaling. The subject and covariate effects were estimated with the general linear model at each voxel. The resulting sets of t values constituted SPMs (SPM{t}). The SPM{t} were transformed to the unit normal distribution (SPM{Z}) and thresholded at $P < .001$ with multiple comparisons. A specific region showing rCBF reduction in very early AD determined by this SPM analysis was incorporated into the eZIS as a volume of interest (VOI).

eZIS Analysis in Group 2

An eZIS program[9] for analysis of brain perfusion SPECT images was used in group 2 subjects to discriminate patients with very early AD at

the MCI stage and age-matched healthy volunteers. Each SPECT image of the group 2 subjects after anatomic standardization by using SPM2 with an original Tc99m-ECD template followed by isotropic 12-mm smoothing was compared with the mean and SD of SPECT images of healthy controls that had already been incorporated in the eZIS program as a normal data base. Voxel-by-voxel *Z*-score analysis was performed after voxel normalization to global mean values: *Z*-score = [(control mean) − (individual value)]/(control SD). The normal SPECT data base of the eZIS program was constructed by using camera 1. It partially duplicated healthy controls in group 1 and comprised a middle-aged group (40–59 years of age, 19 men and 11 women), an older aged group (60–69 years of age, 18 men and 22 women), and an oldest aged group (70–86 years of age, 20 men and 20 women). The appropriate group of these 3 was used as a normal data base to match the age of a subject. The *Z*-score maps were displayed by overlay on tomographic sections and by projection with an averaged *Z*-score of 14-mm thickness to surface rendering of the anatomically standardized MR imaging template. A 3D conversion map calculated from phantom experiments[7] yielded converted SPECT data from camera 2, camera 3, or camera 4 to the core SPECT data from camera 1. As a consequence, 43 of 80 SPECT data were converted to the core SPECT data.

Three indicators for characterizing rCBF decreases in patients with very early AD were determined: First, the severity of rCBF decrease in a specific region showing rCBF reduction in very early AD was obtained from the averaged positive *Z*-score in the VOI. Second, the extent of a region showing significant rCBF reduction in the VOI was obtained—that is, the percentage rate of the coordinates with a *Z* value exceeding the threshold value of 2. Third, the ratio of the extent of a region showing significant rCBF reduction in the VOI to the extent of a region showing significant rCBF reduction in the whole brain was obtained—that is, also the percentage rate of the coordinates with a *Z* value exceeding the threshold value of 2. This ratio indicates the specificity of the rCBF reduction in the VOI compared with that of the whole brain. These 3 indicators were obtained under 2 conditions, with or without data conversion to the core SPECT data by using phantom experiments.

Using the values of the 3 indicators as the threshold, we determined receiver operating characteristic (ROC) curves by using the ROCKIT 0.9β program developed by Metz et al (http://xray.bsd.uchicago.edu/krl).[15] The program calculates the area under the ROC curves (A_z), accuracy, sensitivity, and specificity. Accuracy was determined as the value at the point at which the sensitivity is the same as the specificity on the ROC curve. Then by using the PlotROC program (http://xray.bsd.uchicago.edu/krl), we also statistically calculated the interpolated values for drawing ROC curves.

Results

In group 1, the SPM2 analysis demonstrated significant declines of rCBF of patients with very early AD in the left (−8 −29 36, x y z; *Z* = 4.55) and the right (4 −29 35, x y z; *Z* = 4.21) posterior cingulate gyri, the left (−10 −54 38, x y z; *Z* = 6.1) and the right (6 −62 40, x y z; *Z* = 5.24) precunei, and the left (−44 −66 38, x y z; *Z* = 5.77) and the right (51 −58 45, x y z; *Z* = 5.91) inferior parietal cortices (Fig 1). These areas were registered to eZIS as a specific VOIs.

With data conversion to the core SPECT data, 3 indicators for automated discrimination between patients with very early AD and healthy controls were obtained in group 2 subjects. Healthy controls and patients with AD showed 0.93 ± 0.31 and 1.63 ± 0.48 for severity, 6.32 ± 7.47% and 29.73 ± 18.72% for extent, and 1.84 ± 2.53 and 4.61 ± 2.52 for ratio, respectively. Significant differences (Student *t* test, $P < .001$) were obtained between patients with very early AD and healthy controls.

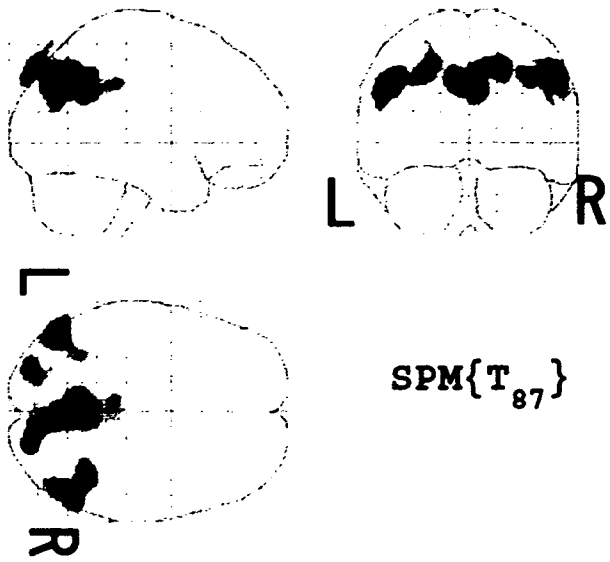

Fig 1. Maximum intensity projections of SPM2 results from group comparison of rCBF between patients with very early AD and age-matched healthy volunteers. Patients with very early AD showed significant decline of rCBF in bilateral posterior cingulate gyri, precunei, and inferior parietal cortices. Height threshold is <0.001, corrected for multiple comparisons.

Without data conversion to the core SPECT data, healthy controls and patients with AD showed 0.85 ± 0.28 and 1.51 ± 0.41 for severity, 3.23 ± 4.07% and 22.06 ± 14.80% for extent, and 1.78 ± 3.00 and 4.68 ± 3.30 for ratio, respectively.

With data conversion to the core SPECT data, the ROC analysis showed A_z values of 0.924, 0.934, and 0.862 for severity, extent, and ratio, respectively (Fig 2). Accuracies for discrimination between healthy controls and patients with very early AD were 85%, 86%, and 80%, respectively. Cutoff values for discrimination were 1.19, 14.2%, and 2.22 for severity, extent, and ratio, respectively.

Without data conversion to the core SPECT data, the ROC analysis showed A_z values of 0.901, 0.911, and 0.828 for severity, extent, and ratio, respectively. Accuracies for discrimination between healthy controls and patients with very early AD also decreased to 82%, 84%, and 75%, respectively.

A representative case of a 78-year-old man with very early AD with an MMSE score of 24 is shown in Fig 3.

Discussion

AD is the most common cause of progressive degenerative dementia that results in global cognitive deterioration, behavioral disturbances, and diffuse cortical atrophy associated with neuronal degeneration. The fact that recent medications like cholinesterase inhibitors delay the progression of AD has increased the importance of diagnosis of AD at the earliest possible stage. In terms of the early diagnosis of AD, the role of functional neuroimaging has become very important as a surrogate marker for the pathologic changes that underlie AD.

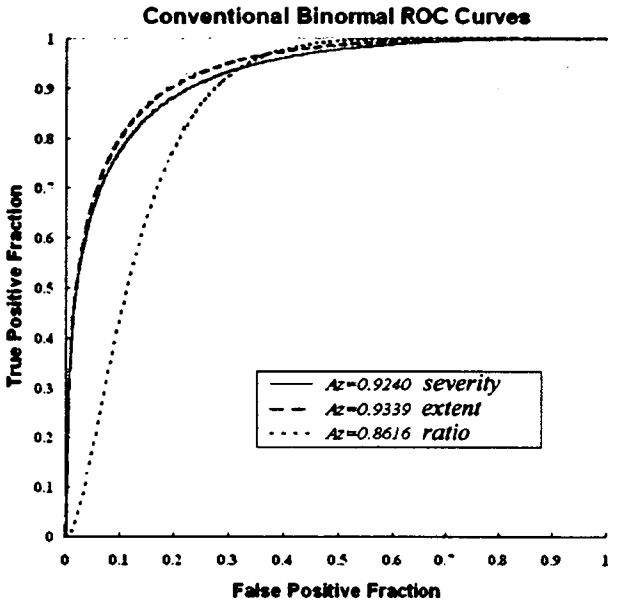

Fig 2. ROC curves with data conversion to the core SPECT data for discrimination between patients with probable AD at the very early stage of MCI and age-matched healthy volunteers in a multicenter study by using the 3 indicators of severity, extent, and ratio.

In our previous study on discrimination of patients with very early AD and age-matched healthy volunteers by using 3D-SSP analysis,[5] the A_z value in the posterior cingulate gyrus and precuneus obtained from ROC analysis was 0.937 with the reference region of global mean counts. The present result of 0.934 in the automated measurement of extent in the VOI was almost equal to that in the previous study. Considering that the number of patients with AD was almost twice that of the previous study and the SPECT images were collected from different institutions with different cameras, we believe that this A_z value would be sufficiently high. This value also compared favorably with the A_z value of 0.930 in a multicenter study using [^{18}F]luorodeoxyglucose PET (FDG-PET)[16] for discrimination of very mild AD using the MMSE scores of more than 24 from healthy controls. This comparable result between PET and SPECT might rather be expected despite the fact that superiority of PET over SPECT has been reported in detecting functional abnormalities in the AD brain.[17,18] In direct comparison of statistical analysis of spatially normalized PET and SPECT scans in AD, Herholz et al[19] reported that PET and SPECT provided comparable results for the main finding of temporoparietal and posterior cingulate functional impairment in mild-to-moderate AD, although the distinction between healthy volunteers and patients with AD is more robust and much less sensitive to threshold selection with PET than with SPECT.

In the present study, 3 indicators for characterizing rCBF decreases in very mild AD were developed. Mizumura et al[20] argued that studying the extent of the region of abnormal rCBF that causes functional disorder was more rational than assessing the severity of the rCBF abnormality that reflected local tissue degeneration. Their contention may be supported by the fact that the discrimination power of the extent was slightly higher than that of the severity in the present study. The ratio indicating specificity of rCBF reduction in the VOI compared with the whole brain had the least discrimination power among the 3 indictors. This indicator may be useful for differentiation of AD from other neuropsychiatric diseases manifesting dementia. A further study will be necessary to confirm the utility of this indicator.

In the present study, conversion of 43 of 80 SPECT data to the core SPECT data for sharing of a normal data base raised the discrimination power of very early AD and healthy controls. Most of previous studies on the sharing of a normal data base have addressed only conversion of the reconstructed SPECT/PET counts in regions of interest from 1 physical condition to another.[21-23] Spatially normalized images with a masking process as used in the present study were used in a recent report on sharing of the normal data base for FDG-PET.[16] However, these reports have not converted the SPECT/PET image itself. Because SPECT exhibits greater variations in image quality among different centers than PET, conversion of SPECT images may be necessary for sharing of a normal data base. Degradation of image resolution to that of a worse image by spatial smoothing has been reported to be one of the most important factors for data sharing between different cameras.[21-23] This adjustment was performed in the current study by smoothing all images with an isometric 12-mm FWHM gaussian kernel as described by Herholz et al.[16]

In the eZIS program, voxel-based analysis is performed by using a *Z*-score map calculated from comparison of a patient's data with the control data base in the same manner as in a 3D-SSP method.[24] Anatomic standardization of SPECT images into a stereotactic space is performed by using SPM2. Therefore, this program is made from the combination of 3D-SSP and SPM2. It has been reported that 3D-SSP with 2D surface projection of cortical activities is less sensitive to artifacts derived from incomplete anatomic standardization of brain with localized cortical atrophy.[25] However, a 3D-SSP technique loses information on the 3D location, which SPECT images inherently possess. This program also has an advantage of the capability of incorporation of SPM results into an automated analysis of *Z*-score values as a VOI. A specific VOI can be determined by group comparison of SPECT images of patients with a neuropsychiatric disease with those of healthy volunteers by using SPM.

Finally, we must refer to several study limitations. First, in the present study, other types of dementia, such as vascular- and frontotemporal-type dementia, were not included. However, previous reports demonstrated that the rCBF decrease in the posterior cingulate gyrus and precuneus is highly specific to AD.[26,27] On the other hand, dementia with Lewy bodies (DLB) has been reported to show similar rCBF decrease in this area.[28] Therefore, although the special emphasis on the decrease of rCBF in this area is reasonable for early diagnosis of AD, this finding may not exclude the possibility of DLB. Second, the onset age of AD was disregarded in the present study. Several studies with PET and SPECT have demonstrated differences in metabolic or rCBF abnormalities between an early onset and late onset of AD.[29,30] Early-onset AD showed more severe metabolic or rCBF decreases in the posterior cingulate cortex, precunei, and parietal cortices than did late-onset AD. A further study should be undertaken to investigate the necessity of separate VOIs showing a rCBF decrease for early-onset and late-onset AD. Third, we retrospectively investigated am-

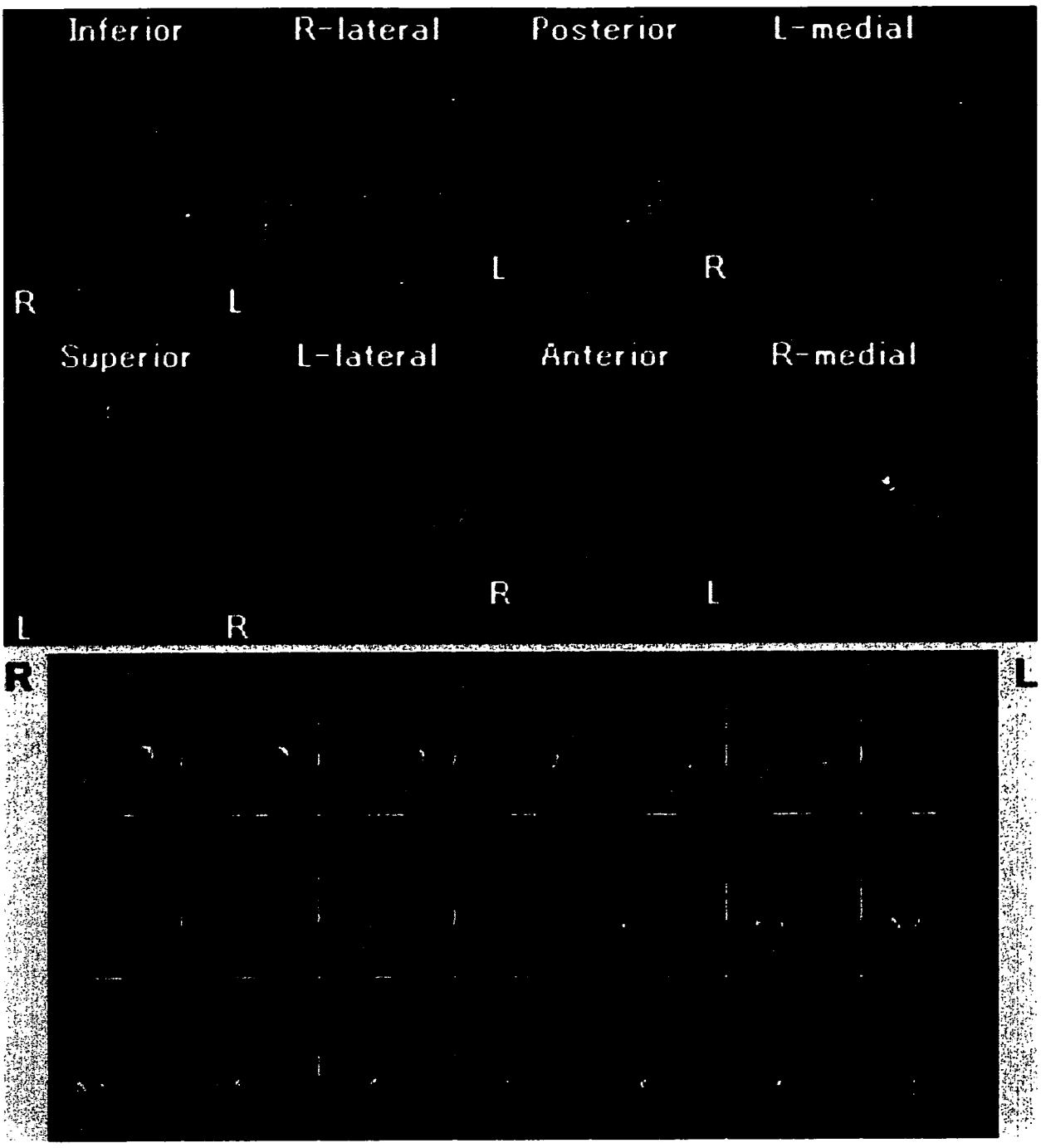

Fig 3. Automated voxel-by-voxel *Z*-score analysis by comparison of a brain perfusion SPECT image of a 78-year-old man with probable AD and an MMSE score of 24 with the mean and SD of SPECT images of healthy volunteers after normalization to global mean cerebral blood flow values. Color-scaled *Z*-score maps ranging from 2.0 to 5.0 with extent threshold of 300 voxels are displayed by overlaying on transaxial sections and surface rendering of the spatially normalized MR imaging template. Red lines enclose a VOI with the most significant decline of rCBF in very early AD obtained from group comparison with healthy volunteers by SPM2. The severity, extent, and ratio are 2.18, 77.2%, and 3.56, respectively.

nestic patients with MCI who all converted to AD. The outcome for any patient with MCI is uncertain because many subjects may remain stable or even revert to a normal state, whereas others progress to dementia. Accordingly, the predictive study using this approach is much more important for MCI conversion to AD. In our previous study,[31] converters from MCI to AD showed a wider area of decreased rCBF prominently in precunei and parietal cortices at the initial SPECT study than nonconverters. The present approach using new indicators for rCBF reductions in these areas would be quite useful for predicting outcomes of patients with MCI.

Conclusion

The automated analysis of brain perfusion SPECT by using eZIS with incorporation of a VOI related to very early AD revealed high performance in discriminating patients with very early AD at the stage of MCI and age-matched healthy volunteers. Moreover, a common normal data base is available